Hindawi
Mathematical Problems in Engineering
Volume 2020, Article ID 4912978, 25 pages
https://doi.org/10.1155/2020/4912978

*Research Article*

# Extended SQ-Coons Surface and Its Application on Fairing Automobile Surface Design

**Fan Liu**,[1] **Xiaomin Ji**,[2,3] **and Jing Gao**[2]

[1]*College of Design and Art, Shaanxi University of Science and Technology, Xi'an 710021, China*
[2]*School of Mechanical and Precision Instrument Engineering, Xi'an University of Technology, Xi'an 710048, China*
[3]*School of Art and Design, Xi'an University of Technology, Xi'an 710054, China*

Correspondence should be addressed to Xiaomin Ji; jixm@xaut.edu.cn

Received 29 May 2020; Revised 6 September 2020; Accepted 28 September 2020; Published 29 October 2020

Academic Editor: Kuei-Hu Chang



Aiming at car design, a parametric design method is proposed in this paper. There are two contents in this method, a novel parametric surface, a shape-adjustable automobile styling template, and a design method of integrating the two contents. The surface termed extended SQ-Coons surface constructed in this paper has the advantage of being fine adjusted while always interpolating at the given boundary curves, which is suitable for its application in automobile modeling design. Matching with the surface, a car model template built by multiple quadrilateral surfaces is proposed. The car models built by the template could achieve the parametric adjustability of all modeling features on the premise of maintaining $G^1$ continuity between subsurfaces. Finally, after the integration of the surface and the template, a whole set of parametric automobile surface modeling design method is proposed. In this method, the overall shape of the car body is determined through multi angle hand drawing, and curve control points, segmentation parameters, and shape parameters are used to adjust the detail modeling. The final results show that the novel surface and template proposed could be used to parametrically establish the vehicle models of various shapes and improve the design efficiency in the conceptual design stage.

## 1. Introduction

For more than 100 years on the market, the social significance of automobile, a typical consumer industrial product, has been no longer limited to the tool attribute of transportation equipment but has given more symbolic significance of life quality and wealth status with the development of the times. With the increasingly fierce competition in the automotive industry, the car body styling design, which directly affects its market performance and brand competitiveness, is highly valued by the whole industry [1]. Modern automobile modeling design could be divided into several levels, such as overall scale and proportion planning, contour line and surface design, detail design adjustment, and so on. Among them, scale proportion design and contour design play an indispensable role because they are directly related to automobile conceptual modeling and directly affect the market performance of automobile products. Compared with the traditional design process, which is a design mode with long design cycle and complex modification process, it has become an inevitable choice and research hotspot to build the mathematical model of vehicle surface by using CAGD (Computer Aided Geometric Design) technology.

CAGD is based on curve and surface modeling technology, including a series of parametric curve and surface theory. Among them, the most famous parametric surfaces could be divided into two types: Bézier-type surface and Coons-type surface. Bézier surface was first proposed in the 1970s, by which a unique curve could be generated through several control points and the shape could be controlled. On this basis, B-spline surfaces and NURBS surfaces, which are widely used in the field of software, have been proposed one after another [2]. In recent years, in order to improve the adjustment ability of surface local shape and to meet the requirements of modern industrial products for surface

modeling, researchers proposed a series of novel Bézier-type surface by introducing the shape parameters [3–8]. Qin et al. [9] have put forward cubic CE-Bézier curve with two shape parameters and its bicubic surface form CE-Bézier surface with four shape parameters, which make the curve and surface have stronger shape adjustment. In the following further research [10], they extended CE-Bézier curve and surface from cubic and bicubic to $n$-degree curve family (with $n-1$ shape parameters) and $m \times n$-degree surface family (with $m+n-2$ shape parameters), respectively, which enhanced the adjustment flexibility and design practicability. After extending the classical Bernstein basis function and introducing global and local shape parameters, Hu et al. [11] constructed the shape-adjustable generalized Bézier (SG-Bézier) curve and surface. In the next research [12, 13], they studied the geometric properties of SG-Bézier curve (e.g., the conditions of continuity between curves, the smoothing method for curves, and the influence of shape parameters on its modeling). In addition, a series of other novel Bézier-type curve and surface have been established by researchers, including $\lambda$-Bézier [14, 15], H-Bézier [16], cubic trigonometric B-spline [17, 18], $\alpha\beta\gamma$-Bernstein–Bézier basis with three exponential additional parameters [19], generalized Bézier-like curves [20], rational quadratic trigonometric Bézier curve [21], and NUAHT B-spline curve [22]. The common point of all the above curves and surfaces is that the shape parameters with various types and value ranges are introduced by modifying the basis functions to achieve the purpose of precise control of the modeling. However, there is a defect in the practical application of all Bézier-type surfaces, that is, with the adjustment of shape parameters, the surface edge could not be interpolated into the fixed boundary curves. On the contrary, interpolation on boundary curve is always the important characteristics of another kind of surface, Coons-type surface.

The establishment of Coons-type surface takes a completely different way of thinking and process from Bézier-type surface. The traditional Coons surface was proposed in the early 1960s and divided into two basic types. The first type of Coons surface only interpolates in the given boundary curves and the shape could not be adjusted. By introducing the blending function, the second type could be interpolated on the boundary curves and cross-boundary derivatives. Since then, researchers have proposed a series of functions such as blending functions to generate some novel Coons-type surfaces. Taking trigonometric Hermit basis functions as the blending function, Xie et al. [23] established a new surface with two shape parameters for shape adjustment and the same properties as the second type of Coons surface. In addition, a second-order trigonometric blending function from Wang et al. [24], a blending function with shape parameter $\lambda$ from Pei et al. [25], and a RBF-Hermit function from Zou [26] are used as blending functions to generate various new Coons-type surfaces with parameters, respectively, and they all have similar geometric properties. However, the existing Coons-type surface also has various defects. The first type of basic Coons surface is too simple to be adjusted delicately. Although the shape of the new Coons surface with parameters could be controlled by shape parameters, it has the same requirements as the second type of traditional Coons surface, so it is difficult to be constructed in the actual design [27]. Nevertheless, the process of building a Coons surface by superposition of 3 surfaces is very enlightening, and this study would also construct a novel parametric surface on this basis.

The minimum surface unit of both Bézier-type and Coons-type surfaces is quadrilateral surface, so the main work of the designer in the computer aided design (CAD for short) process is to use multiple quadrilateral surfaces to establish, adjust, and express the product modeling [28–30]. Based on this, a series of design methods were proposed to adapt to some specific shape expression by means of quadrilateral surface segmentation or splicing. Gunpinar and Gunpinar [31] used the cross-section line as the generatrix when designing the shape of the rotating body such as wine glass and wine bottle, and the control points of the cross-section line were adjusted through the corresponding algorithm to achieve the purpose of modifying the whole product shape. This method was extended to the product design process of similar shapes such as automobile hub, simple roof, and yacht hull. Cheutet et al. [32] focused on the "shape surface" or "ridge line" area of car, which is similar to muscle sculpture and causing subtle light and shadow effects at the shoulder line and waist line of the car body. This method studied the continuity relationship between surfaces and could generate sharp or mellow surface details. Guo et al. [33] proposed a new algorithm to automatically transform product CAD model into high-quality grid according to its shape feature line. In addition to 3D model building, the application of CAGD technology in design also includes modeling analysis and trend forecast. Bluntzer et al. [34, 35] defined the BMW car body modeling as seven features and then put forward two hypotheses and three design levels to describe the internal evolution trend of brand features. According to the algorithm based on the product CAD model, Xiong et al. [36] considered that designers could directly affect consumers' psychological feelings through the obvious features in product CAD modeling. Kumar and Sarkar [37] pointed out that the feature description extracted from the historical CAD model could be used to predict the development trend of automobile brand design. The research of other researchers, such as Cluzel et al. [38] and Hyun et al. [39], also confirmed the important role of the CAD model in modeling design and analysis.

On the basis of the existing study above, this research puts forward a new design theory to carry on the automobile modeling design more efficiently. The theory consists of three levels. The first level is the construction of a novel parametric surface (extended SQ-Coons surface), which has the advantages of both Bézier-type and Coons-type, that is, the local shape of the new surface could be adjusted while interpolating the boundary curves. The second level is an automobile modeling template formed by several quadrilateral surfaces, among which all surfaces are $G^1$ continuous with each other. Different vehicle designs could be generated according to the template by adjusting various parameters. The third level is the combination of the novel surface with the model template, and a whole set of design methods to

generate the body surface by hand sketch and to adjust the details is integrated.

This paper is organized as follows. A vehicle model template composed of 25 quadrilateral surfaces is established in Section 2, and a method of adjustable fairing for surfaces is also introduced. The definition and properties of the extended SQ-Coons surface are described in Section 3. In Section 4, an integrated method of automobile modeling design is proposed. At the end of the paper, we give a short conclusion in Section 5.

## 2. Faired Automobile Surface Modeling Template

*2.1. Construction of CAD Template.* In some common design studies, the researchers use the spliced surfaces without considering the continuity to describe the product shape. In a nutshell, the models built by such methods could reflect the styles and trends quickly, by which different models could be generated according to the adjustment of various parameters. However, there is a disadvantage in the models, that is, the surfaces in the models are only $G^0$ continuous with each other.

The important concept of continuity between surfaces has different significance for automobile products and other simple products. For most products, there is little difference between various continuity. Once the detailed modeling or relevant calculation of automobile modeling (such as CFD analysis) is involved, the difference in continuity would lead to totally different results. In addition, the visual appearance of the whole vehicle would be more realistic only when there is a higher continuity between the surfaces. Considering the requirements of calculation, data, and continuity, this study decided to put forward the corresponding method to improve the continuity between the surfaces to $G^1$ continuous, and on this basis, the modeling of the surface interface is hoped to be controlled. In this study, the vehicle surface model in Figure 1 is established, which is composed of 25 quadrilateral surfaces considering the minimum surface units of each common surface type. By adjusting the modeling of subsurfaces in the model, the model could express the common car modeling through a series of modeling changes, so it is defined as a car modeling template. In the initial stage of the template, each subsurface is only $G^0$ continuous with each other, so it is necessary to propose a fairing method for its subsurfaces.

All aspects of the properties and calculation of surface could be regarded as the extension and continuation of curve. Therefore, the curve is taken as an example first to elaborate the idea of this paper. In the face of the problem of two $G^0$ intersecting curves in Figure 2, the traditional fairing method is modifying its control points to change its curve shape, so that it could reach a mutual $G^1$ or $G^2$ continuous modeling state. There is no doubt that this method could satisfy the concept of fairing in its mathematical definition, but in the design practice, the adjustment of curve modeling means the modification of the design intent and original intention, which would bring a series of more complex problems and work. For this reason, another new method which is more practical for the design process is proposed in this study, that is, to segment two curves at their intersection and generate a new curve in the gap caused by the segmentation. When the new curve could reach $G^1$ (or even $G^2$) continuous, respectively, with the two remaining curves after segmentation, the whole curve group could be faired.

When the above method is extended to the surface, for a quadrilateral parametric surface, it contains two $uv$ parameter directions and corresponding parameters. Therefore, it is the most convenient method to segment a surface directly by the isolate line corresponding to the $uv$ parameter, for the isolate line corresponding to any $uv$ parameter is unique and easy to be obtained on the premise of its mathematical model.

As shown in Figure 3(a), the $uv$ parameter range of the surface in both directions is [0, 1]. Now the $u$ parameters $u_0$ and $u_1$ are taken, which meet the requirements of $0 \le u_0 < u_1 \le 1$. The corresponding isolate lines ($u = u_0$ and $u = u_1$) are used to segment the surface, and the part of [$u_0$, $u_1$] is kept; then, the surface in Figure 3(c) could be obtained, which is a subset of the original surface. In addition, as shown in Figure 3(d), the $v$-direction parameters $v_0$ and $v_1$ ($0 \le v_0 < v_1 \le 1$) are used to segment the previously reserved part according to the similar method to obtain a new quadrilateral surface, which is also a subset of the original surface. Finally, the surface obtained by $uv$-direction parameters [$u_0$, $u_1$] and [$v_0$, $v_1$] is defined as the reserved surface of the original surface in this paper, and the four parameters involved in the segmentation process, $u_0$, $u_1$, $v_0$, and $v_1$, are defined as the segmentation parameters.

There is no doubt that different segmentation parameters would result in various shapes of the reserved surface. As shown in Figure 4, when the segmentation parameters $u_0$, $u_1$, $v_0$, and $v_1$ in Figure 4(a) are modified to $u_0'$, $u_1'$, $v_0'$, and $v_1'$ in Figure 4(b), the same initial surface would be segmented four times to obtain different reserved surfaces. These two reserved surfaces are all subsurfaces of the original surface, so they have similarities, but the differences in details would have completely different effects on the surface modeling design on this basis.

The main significance of defining segmentation parameters is to build a method to adjust the surface shape at the junction of two intersecting surfaces, which would cause the transition surfaces with different shapes. As shown in Figure 5(a), two surfaces **P** and **Q** intersect each other by $G^0$ continuity. After the $u$-direction segmentation parameter $u_{P0}$ of surface **P** and $u$-direction segmentation parameter $u_{Q0}$ of surface **Q** in Figure 5(b) are, respectively, used to segment the surfaces, a certain space would be formed between the reserved surfaces formed after the segmentation. In this case, a new surface **R** in Figure 5(c) could be generated here by using the corresponding surface generation algorithm to achieve $G^1$ continuity conditions with surfaces **P** and **Q** at the same time. According to the above, when the values of the segmentation parameters $u_{P0}$ and $u_{Q0}$ are adjusted, the shape of the two reserved surfaces would change, resulting in the corresponding shape change of surface **R**. In this study, surface **R** is defined as transition surface. As shown in Figures 5(d) and 5(e), when the segmentation parameters are

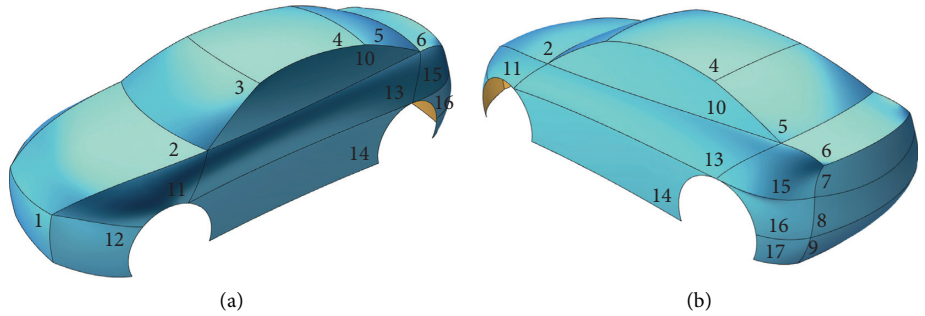


Figure 1: Model template with only $G^0$ continuity between subsurfaces.

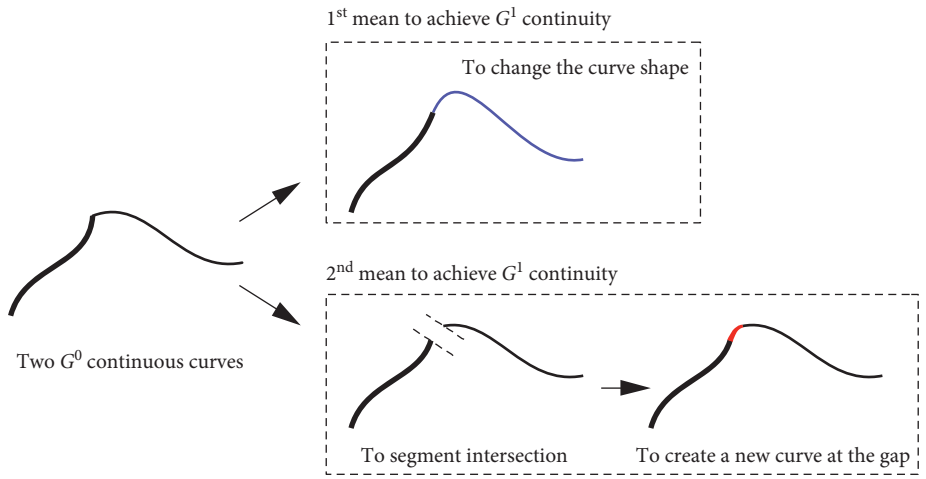


Figure 2: Two methods to improve the continuity between curves.

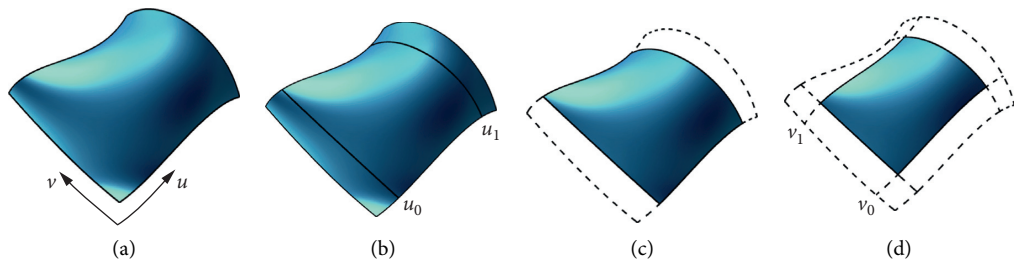


Figure 3: A quadrilateral surface segmented by the isolate lines on corresponding $uv$ parameters. (a) The quadrilateral surface. (b) The isolate lines $u = u_0$ and $u = u_1$. (c) To segment and to keep the $[u_0, u_1]$ region. (d) To segment it on $v$-direction again and to keep the $[v_0, v_1]$ region.

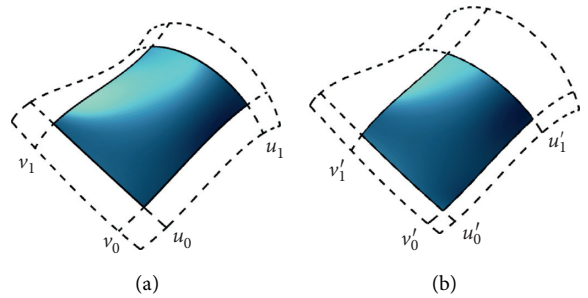


Figure 4: The same surface segmented with various segmentation parameters. (a) Reserved surfaces with the segmentation parameters $u_0$, $u_1$, $v_0$, and $v_1$. (b) Reserved surfaces with the segmentation parameters $u_0{}'$, $u_1{}'$, $v_0{}'$, and $v_1{}'$.

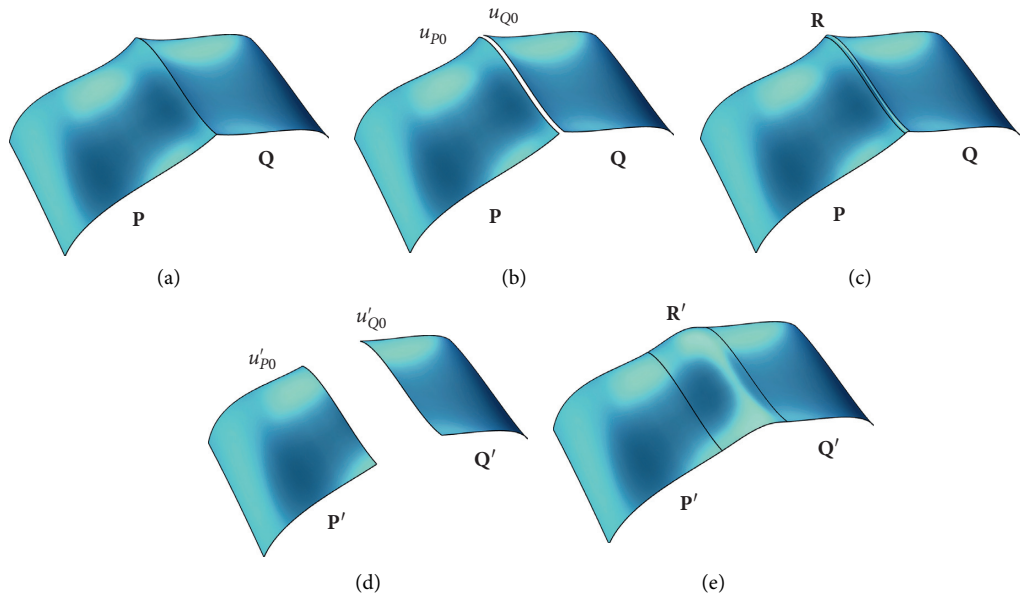


FIGURE 5: Generation and adjustment of transition surface. (a) Two $G^0$ continuous surfaces **P** and **Q**. (b) Segmented by the segmentation parameters $u_{P0}$ and $u_{Q0}$, respectively. (c) Transition surface **R** is generated. (d) Segmented by the segmentation parameters $u_{P0}{}'$ and $u_{Q0}{}'$, respectively. (e) Transition surface **R**′ is generated.

adjusted to $u_{P0}{}'$ and $u_{Q0}{}'$, the shape of the reserved surfaces would change accordingly, and then different spaces between surfaces could be generated, so the final shape of the transition surface built in it is different.

The segmentation and the generation of transition surface between two surfaces are only used for theoretical analysis. For products with complex surface modeling, each subsurface is spliced with the surrounding multi subsurfaces. Ideally, each surface corner is a shared corner of four surfaces so as to maximize the advantages of surface segmentation and transition surface generation. As shown in Figure 6(a), when the surfaces are $G^0$ spliced with each other, each surface joint boundary needs to be segmented and faired. According to the above segmentation method, the surfaces are segmented by segmentation parameters on both sides of the shared boundaries, resulting in an $X$-shaped gap among them, as shown in Figure 6(b). After that, one transition surface is generated between each two surfaces, which could fill the four main branches of the $X$-shaped gap, leaving only one quadrilateral gap in the center. Because the boundary and tangent vector information of the four transition surfaces are determined, a second type Coons surface could be easily generated at the central gap so as to achieve $G^1$ continuity of the whole surface group. In addition, various segmentation parameters would affect the shape of the $X$-shaped gap and then affect the shape of the whole surface group. As shown in Figures 6(e) and 6(f), for the same four original surfaces, different segmentation parameter combinations form the final surface group with different shapes.

This segmentation and transition surface generation method is finally applied to car form design on the template model to generate whole body surfaces of $G^1$ continuity. An automobile model designed according to the template model is illustrated in Figure 7(a), in which the surfaces are $G^0$ continuous with each other, and their shapes have been determined according to the design requirements; in Figure 7(b), each surface is segmented by 2–4 segmentation parameters according to its various position in the model; several transition surfaces marked by dark gray in Figure 7(c) are generated in the gaps between surfaces, and $G^1$ continuous symmetrical car full body surfaces in Figure 7(d) could be constructed.

*2.2. Special Cases in Surface Blending.* It is worth noting that the method shown in Figure 6 is only applicable when 3 surfaces (e.g., No. 3, No. 4, and No. 10 surfaces in Figure 1) or 4 surfaces (e.g., No. 1, No. 2, No. 11, and No. 12 surfaces in Figure 1) intersect at one vertex. This is because the space between 3 or 4 transition surfaces can be filled by generating a second type Coons surface or a degenerated triangular second type Coons surface. However, the pentagonal or hexagonal space formed by the intersection of 5 or 6 surfaces cannot be filled by generating appropriate surfaces. Because of the complexity and particularity of topological relationship between surfaces in the automobile surface modeling template, some special parts need special treatment.

The bottom of A-pillar is an important part of automobile modeling design, where multiple surfaces (No. 2, No. 3, No. 10, No. 11, and No. 13 surfaces in Figure 1) intersect. As shown in Figure 8, if the 5 surfaces are segmented according to their corresponding segmentation parameters on both sides of each intersection line, a pentagon space would be left in the end, and it is difficult to be filled through the traditional quadrilateral parametric surfaces. Therefore, both sides of the intersection line between No. 11 and No. 13 surfaces are not segmented in this method, that is, the surface seam denoted by the black solid line in Figures 8(a) and 8(b) is retained. At this time, when the

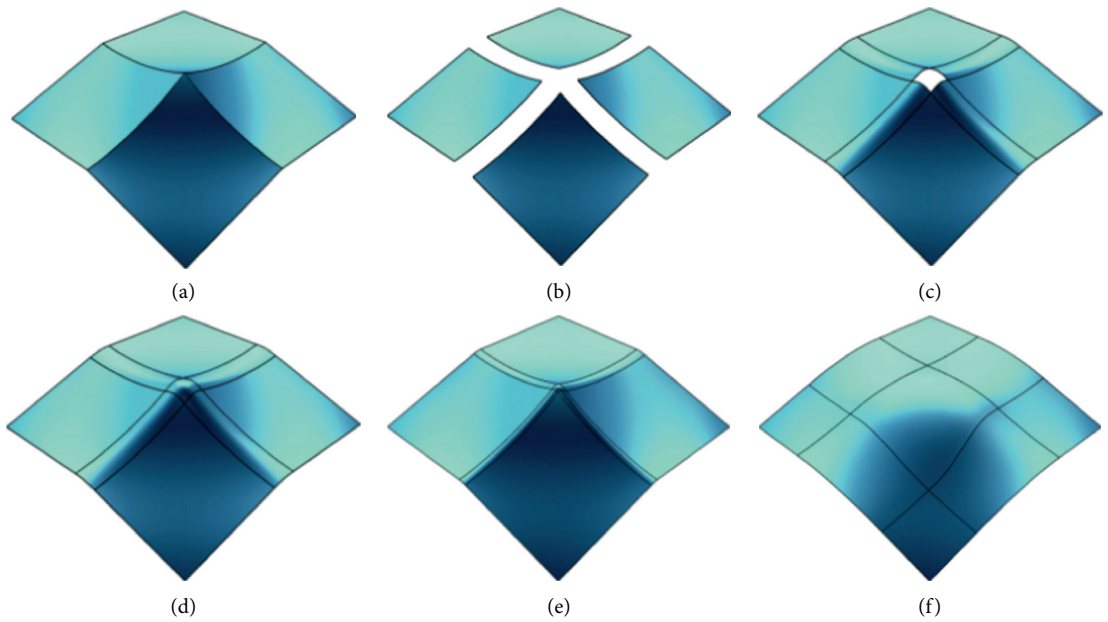


Figure 6: Generation and adjustment of transition surfaces between 4 surfaces. (a)$G^0$ continuous surfaces. (b) Each surface is segmented. (c) Transition surfaces are generated. (d) Vertex transition surface is generated. (e) Different transition surfaces from segmentation parameter 1. (f) Different transition surfaces from segmentation parameter 2.

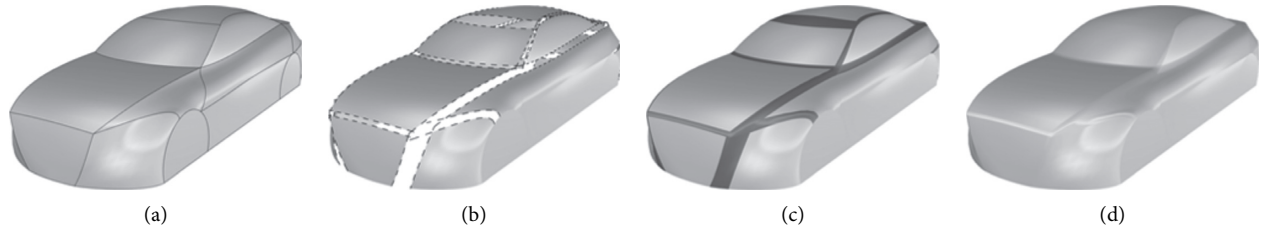


Figure 7: The process to achieve $G^1$ continuity of the whole car body surfaces. (a) The car model adjusted. (b) Segmented by segmentation parameters. (c) The transition surfaces are constructed. (d) The final designed model.

surface group is faired according to the above method, only the quadrilateral space shown in Figure 8(c) is generated, where the space can be filled directly according to the method described in Section 2.1 (see Figure 8(d)).

The same method is also applicable to the bottom of C-pillar. As shown in Figures 9(a) and 9(b), when the joints of No. 13 and No. 15 surfaces are not segmented, the local surface group would also achieve $G^1$ continuity by the generation of transition surface in Figures 9(c) and 9(d).

Since the corresponding individual surfaces in the two local surface groups of Figures 8 and 9 are not segmented, there is no transition surface generation, and the continuity between the two groups of surfaces does not change. Therefore, in order to ensure $G^1$ continuity between subsurfaces of the whole vehicle model template model, the two sets of surfaces (No. 11–No. 13, and No. 13–No. 15) must always be continuous, that is, before the template establishment and segmentation, the two sets of surfaces should be set as always $G^1$ continuous. In addition, since there is no segmentation at the 2 junctions of the 3 surfaces, it is necessary to ensure that the upper edges of the three subsurfaces (No. 11, No. 13, and No. 15) connected at the end keep continuous, so as to make them consistent with other surfaces on the upper side. Therefore, the segmentation parameters in the upper edges of the three surfaces should be set to the same. As shown in Figures 10(a) and 10(b), since the three surfaces have the same span value range [0, 1] and the same boundary curve length in the vertical direction at the junction, when the same upper side segmentation parameters are used for segmentation, the upper side can still keep continuous. At this time, the $G^1$ continuous surface group in Figure 10(c) can be generated during the following fairing operation.

At this point, the car body CAD template with the continuity between surfaces is established. The surface segmentation and transition surface generation methods in this section are only qualitative description, and the specific algorithm for special surface types would be proposed in the next section.

## 3. Extended SQ-Coons Surface

In Section 2 of this paper, the fairing method between the subsurfaces of the whole vehicle is a qualitative analysis

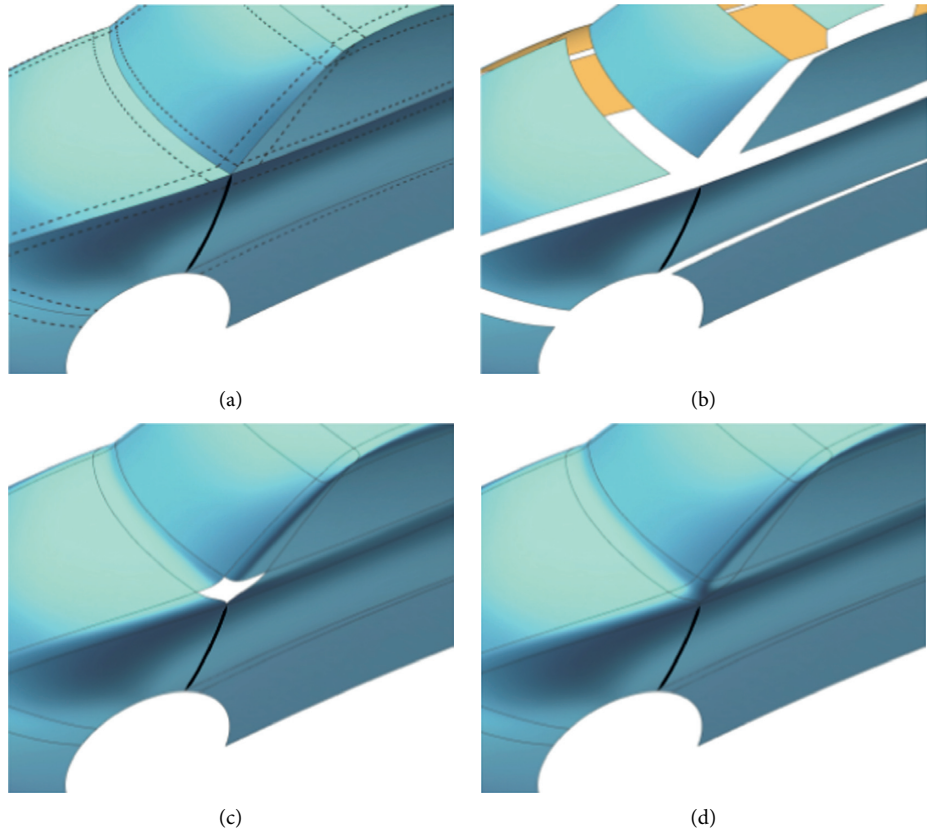


Figure 8: Special treatment of fairing between surfaces at the bottom of A-pillar. (a) Segmentation parameters on both sides of the black junction curve are not set. (b) Surfaces on both sides of the black junction curve are not segmented. (c) After the transition surface is established, a quadrilateral space is generated. (d) After the vertex transition surface is established, the continuity of the whole surface group is achieved.

approach, without emphasizing the specific surface types. However, in order to maximize the advantages of the car body surface template in the modeling design and to improve the adjustability of the automobile surface, a novel surface, extended SQ-Coons (shape-adjustable quasi-Coons) surface is proposed and chosen to describe all the subsurfaces in the body.

*3.1. Mathematical Definition.* The first type of Coons surface is built by superposition of three special surfaces and thus interpolated on the boundary curves. The extended SQ-Coons surface proposed in this paper is also built on the basis of the superposition process, and the surface shape could be adjusted by introducing GE-Bézier basis function. As shown in Figure 11, three special surfaces ($\mathbf{R}_1$, $\mathbf{R}_2$, and $\mathbf{T}$) need to be built in the process of generating extended SQ-Coons surface, and the 3 surfaces are built by four boundary curves and corresponding GE-Bézier shape parameters in different forms.

The basis functions of GE-Bézier curve and surface are proposed by Qin et al. [10]. According to the parity of degree $n$, the expression of GE-Bézier basis function is different. When $n$ is even:

$$G_{i,n}(t) = \begin{cases} \left(C_{n-1}^{i} - \lambda_i t + \lambda_{i-1}(1-t)\right)(1-t)^{n-1-i}t^i & i = 0, 1, \ldots, \dfrac{n}{2} - 1, \\ 2\lambda_{i-1}(1-t)^i t^i & i = \dfrac{n}{2}, \\ \left(C_{n-1}^{i-1} + \lambda_{i-1}t - \lambda_{i-2}(1-t)\right)(1-t)^{n-i}t^{i-1} & i = \dfrac{n}{2} + 1, \ldots, n, \end{cases} \tag{1a}$$

in which there are $n-1$ shape parameters in total, and the range is

$$\lambda_{n/2-1} \in \left[0, C_{n-1}^{n/2-1}\right], \tag{1b}$$

and when $i = 0, 1, 2, n/2-2$:

$$\lambda_{n-2-i}, \lambda_i \in \left[-C_{n-1}^{i+1}, C_{n-1}^{i}\right], \tag{1c}$$

in which $\lambda_{-1} = \lambda_{n-1} = 0$.

When $n$ is odd:

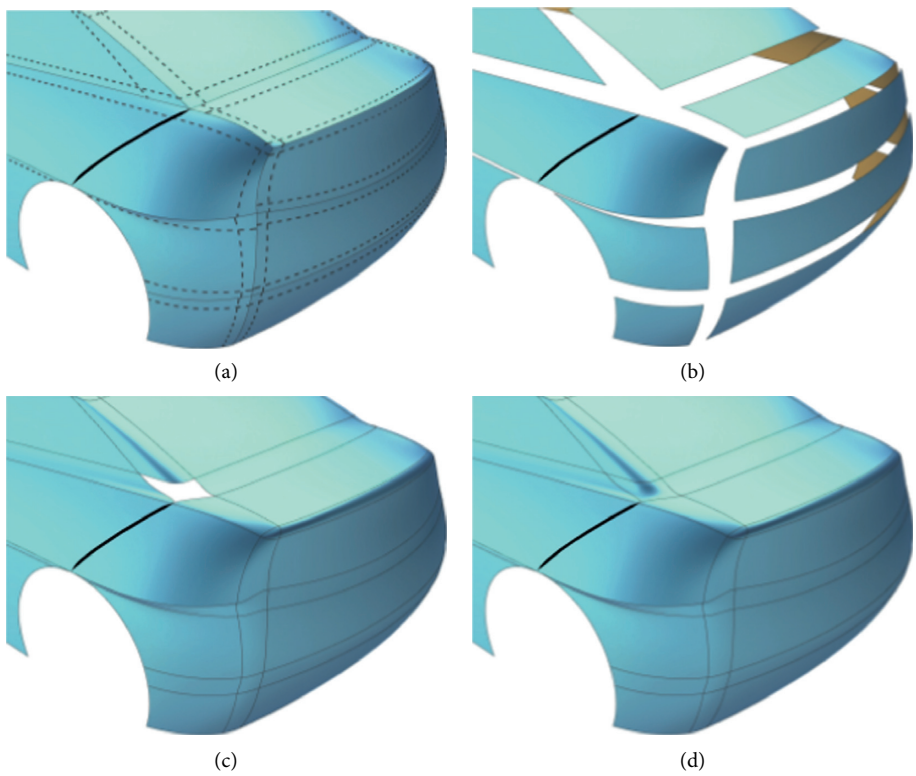


Figure 9: Special treatment of fairing between surfaces at the bottom of C-pillar. (a) Segmentation parameters on both sides of the black junction curve are not set. (b) Surfaces on both sides of the black junction curve are not segmented. (c) After the transition surface is established, a quadrilateral space is generated. (d) After the vertex transition surface is established, the continuity of the whole surface group is achieved.

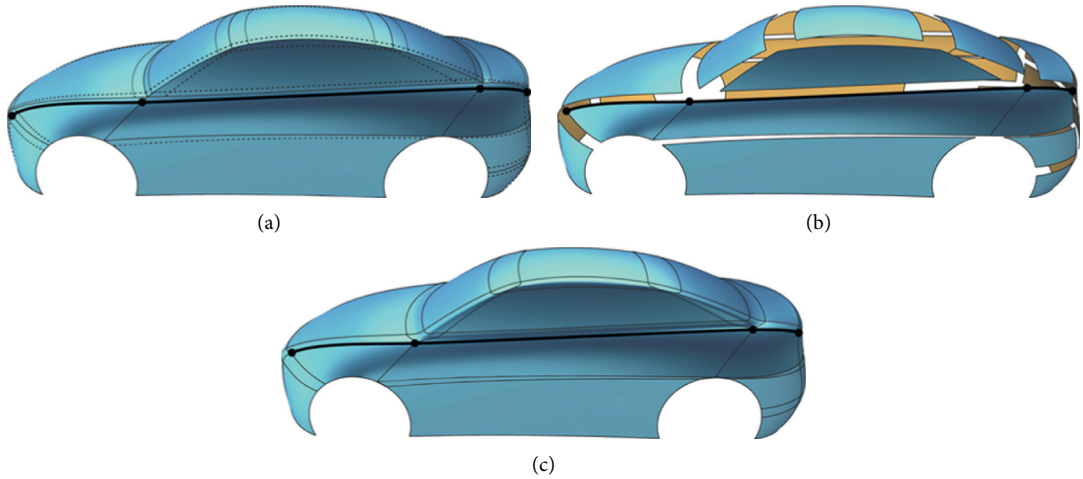


Figure 10: Continuity between surfaces No. 11, No. 13, and No. 15. (a) When the model is established, the continuity of the 3 surfaces is guaranteed. (b) Continuous upper edges are obtained by using the same segmentation parameters. (c) After the transition surface is established, the continuity of the whole surface group is achieved.

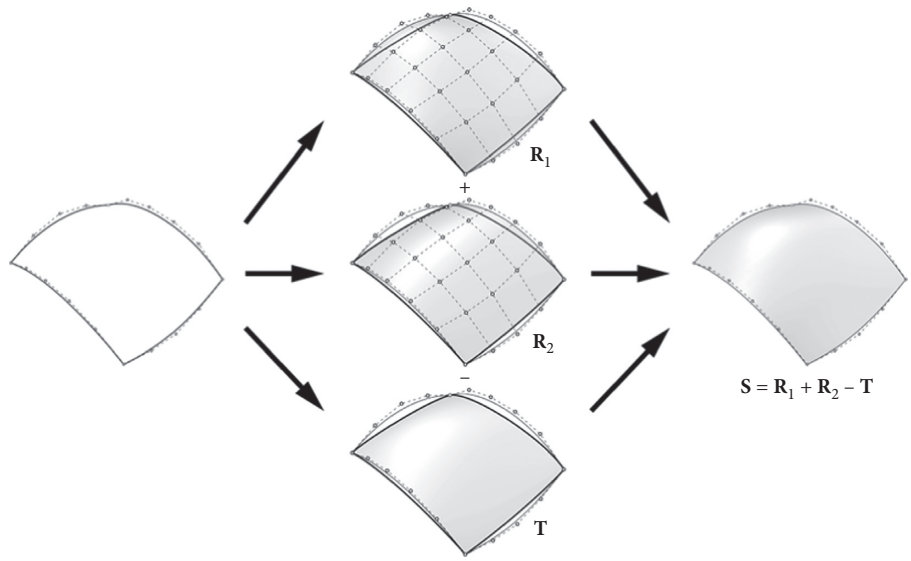


Figure 11: The establishment process of extended SQ-Coons surface.

$$G_{i,n}(t)=\begin{cases}\left(C_{n-1}^{i}-\lambda_i t+\lambda_{i-1}(1-t)\right)(1-t)^{n-1-i}t^{i} & i=0,1,\ldots,\dfrac{n-1}{2}-1,\\ \left(C_{n-1}^{(n-1)/2}+\lambda_{i-1}\right)(1-t)^{n-i}t^{i} & i=\dfrac{n-1}{2},\dfrac{n+1}{2},\\ \left(C_{n-1}^{i-1}+\lambda_{i-1}t-\lambda_{i-2}(1-t)\right)(1-t)^{n-i}t^{i-1} & i=\dfrac{n+1}{2}+1,\ldots,n,\end{cases} \tag{2a}$$

in which there are $n-1$ shape parameters in total, and the range is

$$\lambda_{n-1/2},\lambda_{n-3/2}\in\left[C_{n-1}^{n-1/2},C_{n-1}^{n-3/2}\right], \tag{2b}$$

and when $i=0,\ 1,\ 2,\ (n-1)/2-2$:

$$\lambda_{n-2-i},\lambda_i\in\left[-C_{n-1}^{i+1},C_{n-1}^{i}\right], \tag{2c}$$

in which $\lambda-1=\lambda n-1=0$.

When the basis function has been determined, the novel surface could be established. The input parameters required for the establishment of these three special surfaces are all surface control points, while the input parameters of extended SQ-Coons surface are only control points in boundary curves. Therefore, it is necessary to convert the control points through the establishment of a first type Coons surface.

There are four closed traditional Bézier curves, $\mathbf{p}_{u0}$, $\mathbf{p}_{u1}$, $\mathbf{p}_{v0}$, and $\mathbf{p}_{v1}$, which are connected end-to-end. Among them, the control points of $m$-degree curves $\mathbf{p}_{u0}$ and $\mathbf{p}_{u1}$ are, respectively, $\mathbf{p}_{00}$, $\mathbf{p}_{10}$,. . ., $\mathbf{p}_{m0}$ and $\mathbf{p}_{0n}$, $\mathbf{p}_{1n}$,. . ., $\mathbf{p}_{mn}$, and the control points of $n$-degree curves $\mathbf{p}_{v0}$ and $\mathbf{p}_{v1}$ are $\mathbf{p}_{00}$, $\mathbf{p}_{01}$,. . ., $\mathbf{p}_{0n}$ and $\mathbf{p}_{m0}$, $\mathbf{p}_{m1}$,. . ., $\mathbf{p}_{mn}$, respectively. The expressions are as follows:

$$\begin{aligned}\mathbf{p}_{u0}&=\sum_{i=0}^{m}B_{i,m}(u)\mathbf{p}_{i0},\\ \mathbf{p}_{u1}&=\sum_{i=0}^{m}B_{i,m}(u)\mathbf{p}_{in},\\ \mathbf{p}_{v0}&=\sum_{j=0}^{n}B_{j,n}(v)\mathbf{p}_{0j},\\ \mathbf{p}_{v1}&=\sum_{j=0}^{n}B_{j,n}(v)\mathbf{p}_{mj},\end{aligned} \tag{3}$$

in which $i=0,\ 1,\ \ldots,\ m$; $j=0,\ 1,\ \ldots,\ n$; and $B_{i,m}(u)$ and $B_{j,n}(v)$ are traditional Bernstein basis functions:

$$B_{i,n}(t)=\frac{n!}{i!\,(n-i)!}t^{i}(1-t)^{n-i}. \tag{4}$$

Then, the expression of the first type Coons surface $\mathbf{P}(u, v)$ enclosed by the four curves is

$$\mathbf{p}(u,v)=-\begin{bmatrix}-1 & u & 1-u\end{bmatrix}\begin{bmatrix}0 & \mathbf{p}_{u0} & \mathbf{p}_{u1}\\ \mathbf{p}_{v0} & \mathbf{p}_{00} & \mathbf{p}_{0n}\\ \mathbf{p}_{v1} & \mathbf{p}_{mn} & \mathbf{p}_{m0}\end{bmatrix}\begin{bmatrix}-1\\ v\\ 1-v\end{bmatrix}. \tag{5}$$

After the surface $\mathbf{P}$ is transformed into a $m\times n$-degree Bézier surface, all of its $(m+1)\ (n+1)$ control points could be calculated by

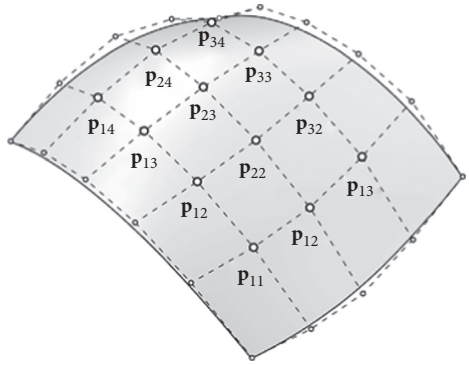


Figure 12: The calculated control points of one extended SQ-Coons surface when $m = 4$ and $n = 5$.

$$\mathbf{p}_{ij} = \begin{bmatrix} \mathbf{p}_{00} & \mathbf{p}_{01} & \cdots & \mathbf{p}_{0n} \\ \mathbf{p}_{10} & \mathbf{p}_{11} & \cdots & \mathbf{p}_{1n} \\ \vdots & \vdots & \ddots & \vdots \\ \mathbf{p}_{m0} & \mathbf{p}_{m1} & \cdots & \mathbf{p}_{mn} \end{bmatrix} = \sum_{i=0}^{m} \sum_{j=0}^{n} \frac{\mathbf{p}(u,v)}{B_{i,m}(u) B_{j,n}(v)}. \quad (6)$$

There are $2(m+n)$ boundary control points (i.e., all control points of curves $\mathbf{p}_{u0}$, $\mathbf{p}_{u1}$, $\mathbf{p}_{v0}$, and $\mathbf{p}_{v1}$) as the initial known data, and the remaining $(m+1)(n+1) - 2(m+n)$ control points in the center of the surface are calculated control points, which means all control points could be obtained from four boundary curves through the above steps. The significance of the calculated control points is that the corresponding $m \times n$-degree Bézier-like surfaces (including the traditional type and the novel type with parameters) could be generated after matching the original boundary curve control points so as to carry out the next operation.

In this paper, two special surfaces $\mathbf{R}_1$ and $\mathbf{R}_2$ are first generated with $\mathbf{p}_{ij}$ as the control point, and their $u$-direction and $v$-direction adopt different curve basis functions. The $u$-direction of the first special surface $\mathbf{R}_1$ follows the traditional Bernstein basis function, and the $v$-direction uses the GE-Bézier basis function. The shape parameters of the $v$-direction GE-Bézier are $\lambda_{v0}, \lambda_{v1}, \ldots, \lambda_{vn}$. This special surface expression is

$$\mathbf{R}_1 = \sum_{i=0}^{m} \sum_{j=0}^{n} B_{i,m}(u) G_{j,n}(v) \mathbf{p}_{ij}. \quad (7)$$

Another surface is a special surface $\mathbf{R}_2$ with GE-Bézier basis function in $u$-direction and Bernstein basis function in $v$-direction. Its shape parameters in $u$-direction are $\lambda_{v0}, \lambda_{v1}, \ldots, \lambda_{vm}$. The expression of surface $\mathbf{R}_2$ is

$$\mathbf{R}_2 = \sum_{i=0}^{m} \sum_{j=0}^{n} G_{i,m}(u) B_{j,n}(v) \mathbf{p}_{ij}. \quad (8)$$

$G_{j,n}(v)$ and $G_{j,n}(u)$ in formulas (7) and (8) are all GE-Bézier basis function formulas from formulas (1a)–(1c) and (2a)–(2c).

The third special surface $\mathbf{T}$ is a first type Coons surface. And its boundary curves are GE-Bézier boundary curves in $v$-direction of surface $\mathbf{R}_1$ and GE-Bézier boundary curves in $u$-direction of surface $\mathbf{R}_2$. These four GE-Bézier curves are named as $\mathbf{p}_{u0}{}'$, $\mathbf{p}_{u1}{}'$, $\mathbf{p}_{v0}{}'$, and $\mathbf{p}_{v1}{}'$, and the expressions are

$$\begin{aligned} \mathbf{p}_{u0}{}' &= \sum_{i=0}^{m} G_{i,m}(u) \mathbf{p}_{0i}, \\ \mathbf{p}_{u1}{}' &= \sum_{i=0}^{m} G_{i,m}(u) \mathbf{p}_{3i}, \\ \mathbf{p}_{v0}{}' &= \sum_{i=0}^{n} G_{j,n}(v) \mathbf{p}_{j0}, \\ \mathbf{p}_{v1}{}' &= \sum_{i=0}^{n} G_{j,n}(v) \mathbf{p}_{j3}. \end{aligned} \quad (9)$$

The first type Coons surface $\mathbf{T}$ is generated by taking the four new GE-Bézier curves as boundary curves, and its expression is as follows:

$$\mathbf{T} = -\begin{bmatrix} -1 & u & 1-u \end{bmatrix} \begin{bmatrix} 0 & \mathbf{p}_{u0}{}' & \mathbf{p}_{u1}{}' \\ \mathbf{p}_{0v}{}' & \mathbf{p}_{00} & \mathbf{p}_{03} \\ \mathbf{p}_{1v}{}' & \mathbf{p}_{30} & \mathbf{p}_{33} \end{bmatrix} \begin{bmatrix} -1 \\ v \\ 1-v \end{bmatrix}. \quad (10)$$

On the basis that special surfaces $\mathbf{R}_1$, $\mathbf{R}_2$, and $\mathbf{T}$ have been built, a new surface $\mathbf{S}$ could be built by referring to the method of the first type Coons surface. The surface $\mathbf{S}$ is the extended SQ-Coons surface proposed in this study, and its superposition algorithm is

$$S = R_1 + R_2 - T. \quad (11)$$

A new extended SQ-Coons surface is created by the above steps. It could be concluded from the whole generation process of the surface that the input parameters needed to build the new surface $\mathbf{S}$ are only the four boundary curves and its GE-Bézier shape parameters in corresponding directions, without additional boundary vector information.

*3.2. Geometric Properties.* The boundary is always interpolated in the given boundary curves, and the middle part of an extended SQ-Coons surface has similar properties with GE-Bézier surface. In short, for the extended SQ-Coons surface with $m = 4$ and $n = 5$ in Figure 12, with the decrease of $\lambda_{u0}$, the overall trend of the surface would gradually move away from the calculated control points $\mathbf{p}_{11}$, $\mathbf{p}_{12}$, $\mathbf{p}_{13}$, and $\mathbf{p}_{14}$, and in contrast, with the increase of $\lambda_{u0}$, it would gradually approach the calculated control points $\mathbf{p}_{11}$, $\mathbf{p}_{12}$, $\mathbf{p}_{13}$, and $\mathbf{p}_{14}$. Similarly, with the decrease or increase of $\lambda_{u1}$, the overall trend of the surface would gradually move away from or near the calculated control points $\mathbf{p}_{21}$, $\mathbf{p}_{22}$, $\mathbf{p}_{23}$, and $\mathbf{p}_{24}$. It also has the same geometric properties in the $v$-direction. In addition, this property could be spread to any degree of extended SQ-Coons surface.

Based on the above, the influence of this property on surface modeling is shown in Figure 13. Because of their same boundary curves, the shape does not vary much under different parameters. Here, the mean curvature nephogram

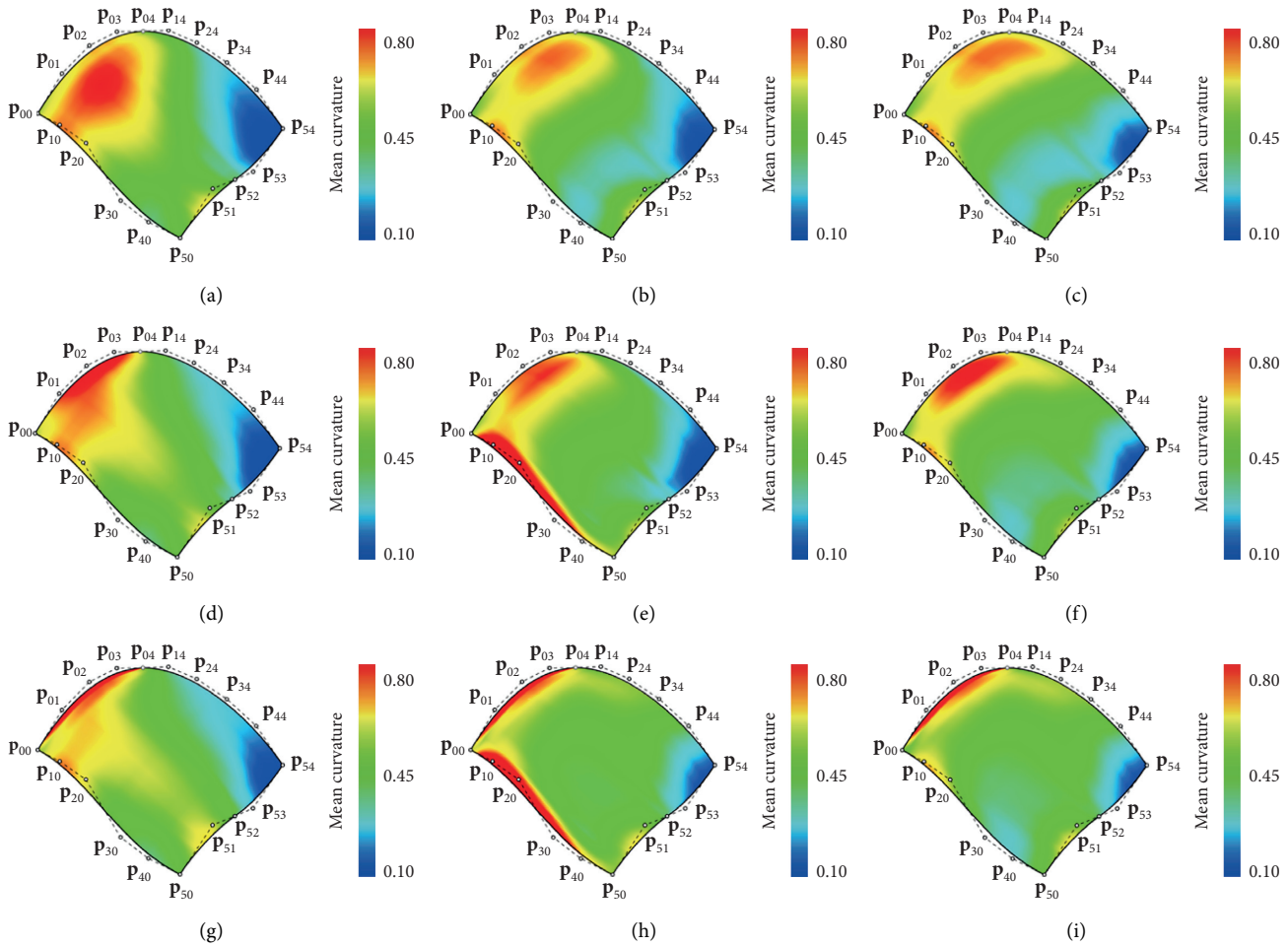


FIGURE 13: Various mean curvatures in nephogram of an extended SQ-Coons surface with different shape parameters. (a) $\lambda_{u0} = 1$, $\lambda_{u1} = 4$, $\lambda_{u2} = 4$, $\lambda_{u3} = 1$; $\lambda_{v0} = 1$, $\lambda_{v1} = 3$, $\lambda_{v2} = 1$. (b) $\lambda_{u0} = 1$, $\lambda_{u1} = 4$, $\lambda_{u2} = 4$, $\lambda_{u3} = 1$; $\lambda_{v0} = -3$, $\lambda_{v1} = 2$, $\lambda_{v2} = 1$. (c) $\lambda_{u0} = 1$, $\lambda_{u1} = 4$, $\lambda_{u2} = 4$, $\lambda_{u3} = 1$; $\lambda_{v0} = -3$, $\lambda_{v1} = 0$, $\lambda_{v2} = 3$. (d) $\lambda_{u0} = -2$, $\lambda_{u1} = 0$, $\lambda_{u2} = -2$, $\lambda_{u3} = 1$; $\lambda_{v0} = 1$, $\lambda_{v1} = 3$, $\lambda_{v2} = 1$. (e) $\lambda_{u0} = 0$, $\lambda_{u1} = 1$, $\lambda_{u2} = -4$, $\lambda_{u3} = 0$; $\lambda_{v0} = -2$, $\lambda_{v1} = 1$, $\lambda_{v2} = 0$. (f) $\lambda_{u0} = -1$, $\lambda_{u1} = -2$, $\lambda_{u2} = 2$, $\lambda_{u3} = -3$; $\lambda_{v0} = -3$, $\lambda_{v1} = 0$, $\lambda_{v2} = -3$. (g) $\lambda_{u0} = -4$, $\lambda_{u1} = -6$, $\lambda_{u2} = -6$, $\lambda_{u3} = -4$; $\lambda_{v0} = 1$, $\lambda_{v1} = 3$, $\lambda_{v2} = 1$. (h) $\lambda_{u0} = -4$, $\lambda_{u1} = -6$, $\lambda_{u2} = -6$, $\lambda_{u3} = -4$; $\lambda_{v0} = -2$, $\lambda_{v1} = 0$, $\lambda_{v2} = 3$. (i) $\lambda_{u0} = -4$, $\lambda_{u1} = -6$, $\lambda_{u2} = -6$, $\lambda_{u3} = -4$; $\lambda_{v0} = -3$, $\lambda_{v1} = 0$, $\lambda_{v2} = 3$.

is needed to show the difference of surface details. The mean curvature is an important concept to describe the shape of a surface, so the nephogram of mean curvature is an intuitive way to visually express its shape. As can be seen in Figure 13, in 9 different shape parameter value combinations, the surface shows different average curvature trends in the middle while maintaining the absolute feature of interpolation in the boundary curve, and the shape trend is only related to shape parameter information.

Table 1 describes the properties of different surface types. Among them, extended SQ-Coons surface is the only surface with shape adjustability, interpolation on boundary curves, and generating process without cross-boundary derivative; in addition, it has the least number of control points. Because of this, extended SQ-Coons surface is very suitable for parametric product modeling design based on surface boundary curves.

*3.3. Establishment of Segmentation Algorithm.* In order to apply the extended SQ-Coons surface to the typical car body template established in Section 2 of this paper, a specific algorithm corresponding to the surface segmentation proposed in Section 2 needs to be established. Since the composition of extended SQ-Coons surface is the superposition of three special surfaces (as described in formula (11), i.e., $\mathbf{S} = \mathbf{R}_1 + \mathbf{R}_2 - \mathbf{T}$), the segmentation process can also be decomposed as shown in Figure 14, that is, the three special subsurfaces are segmented and then superimposed again.

Therefore, the segmentation problem of extended SQ-Coons surface can be transformed into three types of segmentation problems, that is, the segmentation of 2 different directions in $\mathbf{R}_1$ or $\mathbf{R}_2$ (GE-Bézier direction and traditional Bézier direction) and the first type Coons surface represented by the third special surface $\mathbf{T}$. Among them, the segmentation of

Table 1: Temperature and wildlife count in the three areas covered by the study.

| Surface type | Control points | Shape adjustable? | Interpolates boundaries? | Need cross-boundary derivative? |
|---|---|---|---|---|
| Extended SQ-Coons | $2(m+n)$ | Yes | Yes | No |
| Bézier | $m \times n$ | No | Yes | N/A |
| NURBS | $m \times n$ | Yes | Yes | N/A |
| CE-Bézier | $m \times n$ | Yes | No | N/A |
| Coons (1st type) | $2(m+n)$ | No | Yes | No |
| Coons (2nd type) | $2(m+n)$ | No | Yes | Yes |
| Novel Coons-type | $2(m+n)$ | Yes | Yes | Yes |

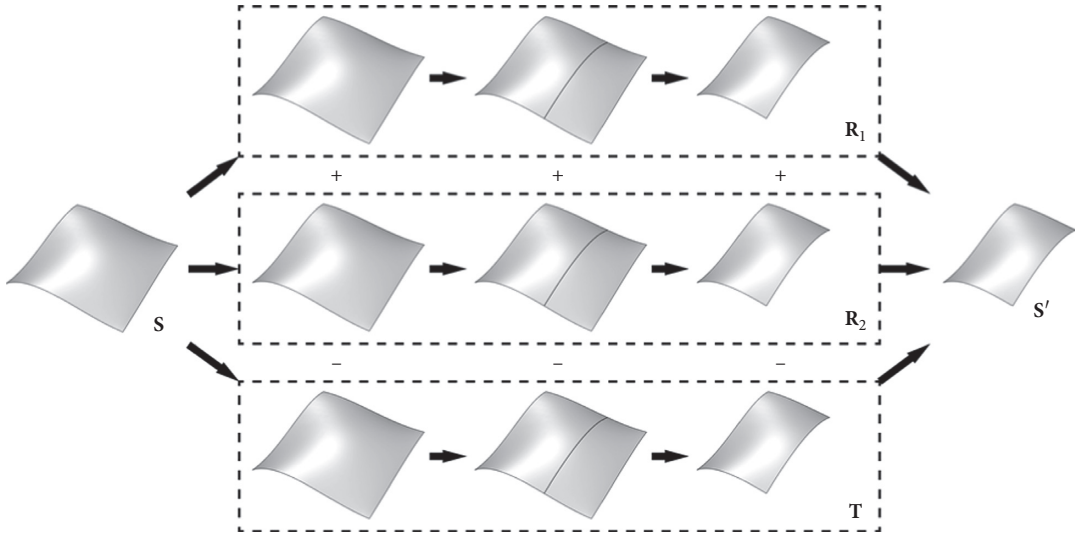


Figure 14: The segmentation of a SQ-Coons surface is decomposed into 3 surfaces.

traditional Bézier surface and first type Coons surface can be transformed into the De Casteljau recursive segmentation algorithm of Bézier curve; therefore, the key in segmentation algorithm of extended SQ-Coons surface is the GE-Bézier surface segmentation method. And the segmentation method of GE-Bézier surface is the generalization of its corresponding parametric curve, so the segmentation algorithm of GE-Bézier curve should be introduced first.

Because the shape of a GE-Bézier curve is determined by its control points and shape parameters simultaneously, its calculation method needs to be specially constructed. Firstly, a GE-Bézier curve $\mathbf{h}$ with degree $n$ defined by control point $\mathbf{h}_i$ ($i = 0, 1, \ldots, n$) and shape parameter $\lambda_i$ ($i = 0, 1, \ldots, n-2$) is generated:

$$\mathbf{h}(t; \lambda_0, \ldots, \lambda_{n-2}) = \sum_{i=0}^{n} G_{i,n}(t)\mathbf{h_i}, \tag{12}$$

and the curve $\mathbf{h}$ is divided into two new GE-Bézier curves $\mathbf{k}$ (with the control points $\mathbf{k}_i$ and shape parameters $\lambda_{ki}$) and $\mathbf{l}$ (with the control points $\mathbf{l}_i$ and shape parameters $\lambda_{li}$) of degree $n$ by a point $\mathbf{h}*$ on $\mathbf{h}$ with $t = t^*$, as illustrated in Figure 15. Then, $\mathbf{k}_n = \mathbf{l}_n = \mathbf{h}^*$, $\mathbf{k}_0 = \mathbf{h}_0$, and $\mathbf{l}_0 = \mathbf{h}_n$.

The expression of curve $\mathbf{h}$ would be expanded, and no matter whether the degree $n$ is odd or even, it can be rewritten as a polynomial of degree $n$ about $t$:

$$\mathbf{h}(t; \lambda_0, \ldots, \lambda_{n-2}) = f_0 + f_1 t + f_2 t^2 + \cdots + f_n t^n, \tag{13}$$

where $f_0, f_1, \ldots, f_n$ are the coefficients about $t^i$ including $\mathbf{h}_i$ and $\lambda_i$, $i = 0, 1, \ldots, n$.

The $[0, t^*]$ part of the original curve $\mathbf{h}$ before segmentation is the curve $\mathbf{k}$ after segmentation, and the segmentation points $\mathbf{h}^*$ are the points with $t = t^*$ on $\mathbf{h}$ and $t = 1$ on $\mathbf{k}$, respectively. Therefore, parameters $t'$ and $t''$ are proposed here, and it can be assumed that the value of any $t'$ in the interval $[0, t^*]$ corresponds to the value of $t''$ on the curve $\mathbf{k}(t)$:

$$t'' = \frac{t'}{t^*}, \quad 0 \le t'' \le 1. \tag{14}$$

Therefore, the parameter of the corresponding parameter segment or the corresponding segmentation point is brought into the curve equation $\mathbf{h}$ and $\mathbf{k}$, respectively, which should be equal:

$$\mathbf{h}(t'; \lambda_0, \ldots, \lambda_n) = \mathbf{k}(t; \lambda_{k0}, \ldots, \lambda_{kn-2}),$$
$$f_0 + f_1 t' + f_2 t^{x\prime 2} + \cdots + f_n t'^n = f_0^* + f_1^* t'' + f_2^* t''^2 + \cdots + f_n^* t''^n, \tag{15}$$

where $f_0^*, f_1^*, \ldots, f_n^*$ are the coefficients about $t''^i$ including $\mathbf{k}_i$ and $\lambda_{ki}$, $i = 0, 1, \ldots, n$.

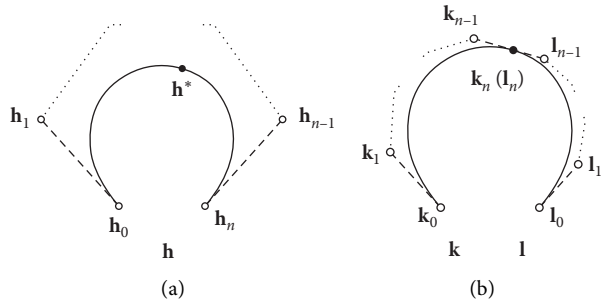


FIGURE 15: Segmentation of a $n$-degree GE-Bézier curve. (a) The original $n$-degree curve $h$. (b) 2 new curves $k$ and l formed by segmentation.

By introducing the setting of $t'$ and $t''$ in formula (14) into formula (15), the expression of $\mathbf{k}_i$ with $\mathbf{h}_i$, $\lambda_i$, and $\lambda_{ki}$ can be obtained. However, for GE-Bézier curve $\mathbf{k}$, its shape is determined by the control points and shape parameters. Therefore, in order to obtain the certain control point data, it is necessary to determine the value of its shape parameters. In addition, in order to simplify the calculation, the shape parameters of GE-Bézier curve after segmentation are determined as the maximum value of its value range, that is to say, the new curve is described by the expression of traditional Bézier curve. This processing makes the new curve have simpler mathematical properties while the shape can be controlled by the shape parameters of the original GE-Bézier curve before segmentation.

The method can also be extended to the segmentation of GE-Bézier surface. As indicated in Figures 16(a) and 16(b), when a $u$-direction parameter is used to segment the GE-Bézier surface $\mathbf{P}$ with $4 \times 2$ degree, the process can be regarded as using this parameter to segment the GE-Bézier curve formed by each group of control points in the direction. The two groups of control points formed after segmentation can construct the new surfaces $\mathbf{Q}$ and $\mathbf{Q}'$, respectively. Similar to the segmentation property of GE-Bézier curve, the $u$-direction of the surfaces $\mathbf{Q}$ and $\mathbf{Q}'$ is constructed according to the traditional Bézier basis function. Therefore, when a $v$-direction parameter in Figures 16(d) and 16(e) is used to segment the surface $\mathbf{Q}$ again, the final preserved surface $\mathbf{R}$ in Figure 16(f) is a surface expressed by the traditional Bézier surface expression. The advantage of this method is that the shape of the surface $\mathbf{R}$ can be adjusted by the shape parameters of the original surface $\mathbf{P}$, and its expression is relatively simple, which is conducive to the following related calculation.

*3.4. Algorithm for Generating Transition Surfaces.* When generating the transition surface between two segmented surfaces, because there are numerous surfaces which can reach the continuity with both sides of the surface, it is necessary to limit the generation algorithm to ensure that the only transition surface is generated.

Firstly, the generation method of transition curve is introduced. As illustrated in Figures 17(a) and 17(b), two cubic curves $\mathbf{P}$ and $\mathbf{Q}$ intersected by $G^0$ are divided into two cubic curves $\mathbf{P}_1$, $\mathbf{P}_2$ and $\mathbf{Q}_1$, $\mathbf{Q}_2$ by the points $\mathbf{p}'$ and $\mathbf{q}'$ on them, respectively. If a new transition curve is generated between $\mathbf{P}_1$ and $\mathbf{Q}_1$ and the transition curve is constructed based on the control points of two subcurves $\mathbf{P}_2$ and $\mathbf{Q}_2$ which are not reserved after segmentation, the curve is unique and the generation method is relatively simple.

As shown in Figure 17(c), the control points of the 2 new curves $\mathbf{P}_2$ and $\mathbf{Q}_2$ are $\mathbf{p}_{2\text{-}0}$, $\mathbf{p}_{2\text{-}1}$, $\mathbf{p}_{2\text{-}2}$, and $\mathbf{p}_{2\text{-}3}$ and $\mathbf{q}_{2\text{-}0}$, $\mathbf{q}_{2\text{-}1}$, $\mathbf{q}_{2\text{-}2}$, and $\mathbf{q}_{2\text{-}3}$, respectively, in which $\mathbf{p}_{2\text{-}0} = \mathbf{q}_{2\text{-}0}$, $\mathbf{p}_{2\text{-}3} = \mathbf{p}'$, and $\mathbf{q}_{2\text{-}3} = \mathbf{q}'$. According to the continuity property of Bézier curve, it can be known that when a new curve and $\mathbf{P}_1$ intersect at $\mathbf{p}'$ and the second control point is on $\mathbf{p}_{2\text{-}3}\mathbf{p}_{2\text{-}2}$ and its extension line, it can reach at least $G^1$ continuity with curve $\mathbf{P}_1$, and the same applies to $\mathbf{Q}_1$. As shown in Figure 17(d), $\mathbf{p}_{2\text{-}3}\mathbf{p}_{2\text{-}2}$ and $\mathbf{p}_{2\text{-}0}\mathbf{p}_{2\text{-}1}$ can be lengthened and can intersect at a new point $\mathbf{p}_2'$, while $\mathbf{q}_{2\text{-}3}\mathbf{q}_{2\text{-}2}$ and $\mathbf{q}_{2\text{-}0}\mathbf{q}_{2\text{-}1}$ can be lengthened and can intersect at a new point $\mathbf{q}_2'$. As shown in Figure 17(e), another new curve $\mathbf{T}$ is generated by the control points $\mathbf{p}_{2\text{-}3}$, $\mathbf{p}_2'$, $\mathbf{q}_2'$, and $\mathbf{q}_{2\text{-}3}$, which is still $G^1$ continuous with $\mathbf{P}_1$ and $\mathbf{Q}_1$. Since the positions of the four control points are certain, the curve $\mathbf{T}$ is unique.

The generation of transition surface follows the same method. As indicated in Figure 18, 2 $G^0$ continuous surfaces $\mathbf{P}$ and $\mathbf{Q}$ are divided into two surfaces $\mathbf{P}_1$, $\mathbf{P}_2$ and $\mathbf{Q}_1$, $\mathbf{Q}_2$, and a new transition surface $\mathbf{T}$ can be generated according to the method described above. In the same way, surface $\mathbf{T}$ and surfaces $\mathbf{P}_1$ and $\mathbf{Q}_1$ are $G^1$ continuous and unique.

So far, all algorithms involved in the application of extended SQ-Coons surface into the CAD template proposed in Section 2 have been introduced. And in the next section, the integrated design method would be expanded.

## 4. Parametric Design Method of Vehicle Surface

In the surface product modeling design, it is an important design method to generate and adjust the surface with the feature line as the main reference and constraint. The advantage of this method is that the shape of the most obvious contour line and feature line in the user's visual perception limits the size and overall shape of the whole product and makes the following surface design and detail adjustment reasonable. At the same time, as a typical application of CAD technology, this method also has high digital requirements for the 3D geometric model involved. The typical car body prototype template proposed in Section 2 of this paper is based on quadrilateral surfaces, the most basic element of parametric geometry, and the extended SQ-Coons surface mathematical model proposed in Section 3 of

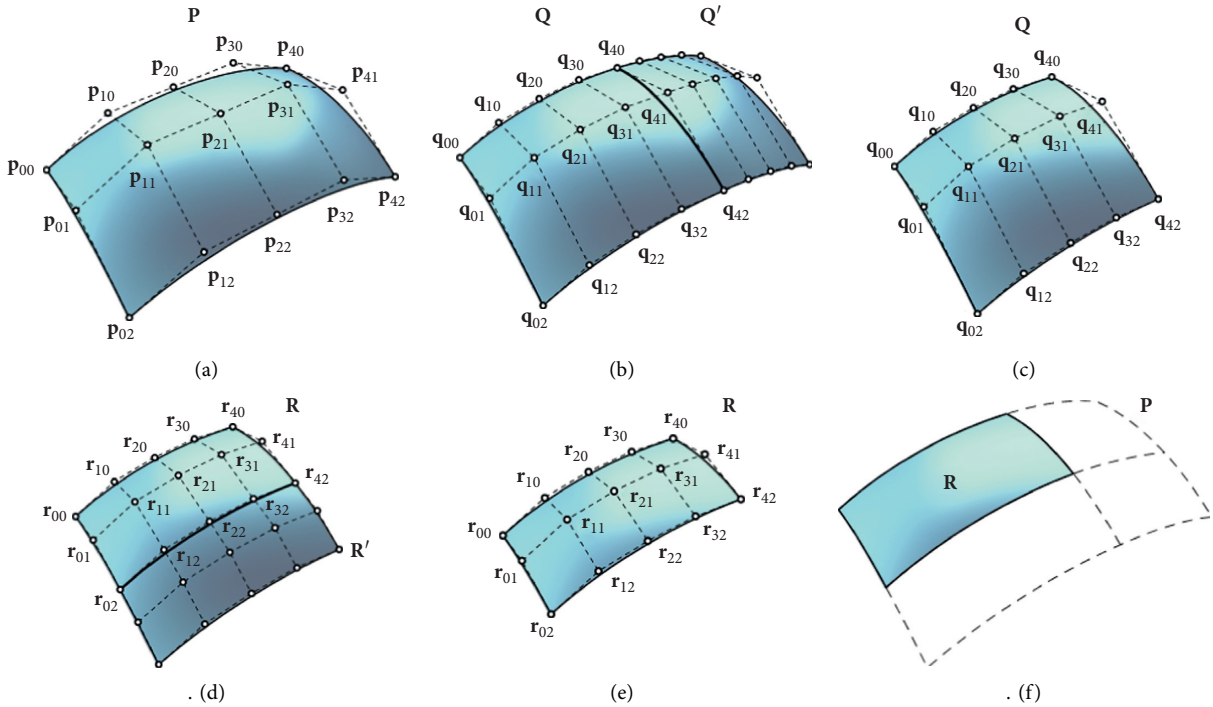


Figure 16: Segmentation of a GE-Bézier surface. (a) A $4 \times 2$-degree GE-Bézier surface $\mathbf{P}$. (b) Segmented into 2 new surfaces. (c) One of the new surfaces is $\mathbf{Q}$. (d) Segmented into 2 new surfaces in the other direction. (e) One of the new surfaces is $\mathbf{R}$. (f) Original surface and the new surface after twice segmentation.

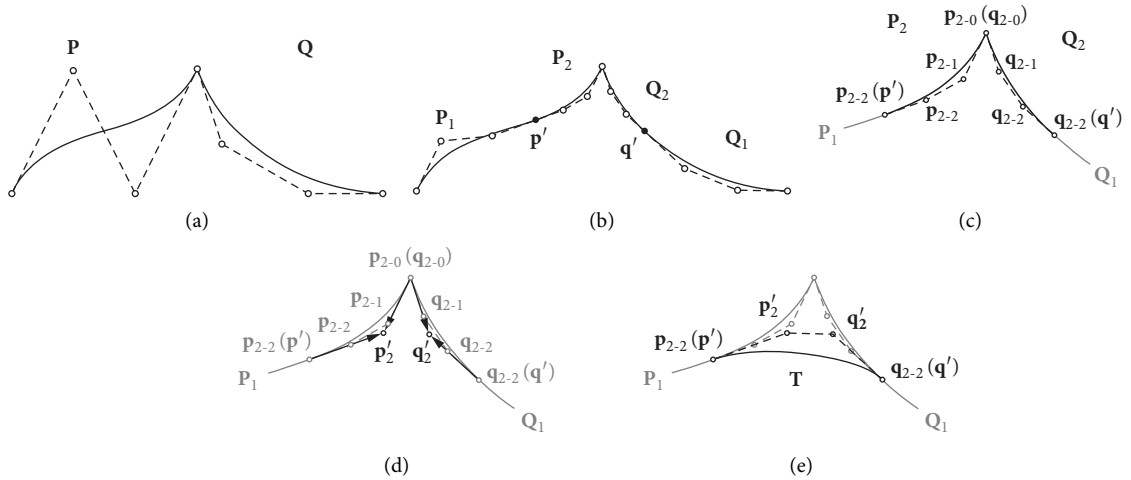


Figure 17: Generating a transition curve between two curves. (a) Curves $\mathbf{P}$ and $\mathbf{Q}$ with $G^0$ continuous. (b) Segmented into two curves $\mathbf{P}_1$, $\mathbf{P}_2$ and $\mathbf{Q}_1$, $\mathbf{Q}_2$, respectively. (c) Control points of curves $\mathbf{P}_2$ and $\mathbf{Q}_2$. (d) The new points $\mathbf{p}_2'$ and $\mathbf{q}_2'$. (e) Establishment of transition curve $\mathbf{T}$.

this paper also fully follows the idea of using feature lines to control the surface modeling and introduces the possibility of adjusting the details on this basis. Therefore, the combination of the two would play their respective advantages, improve the efficiency of modeling design, and explore more design possibilities.

The first step of the design method flow is that after the product modeling feature line is described by hand drawing sketch, effect drawing, and three views, the 3D wireframe of the feature line would be established by corresponding methods. Then, the subcurves form closed quadrilateral in the wireframe, as the first type of input parameters, are used to describe the whole vehicle modeling by establishing extended SQ-Coons surfaces. Each extended SQ-Coons surface could be segmented and faired due to the existence of segmentation parameters to change its transition shape. At the same time, the surface details in each surface could also be adjusted through the built-in shape parameters.

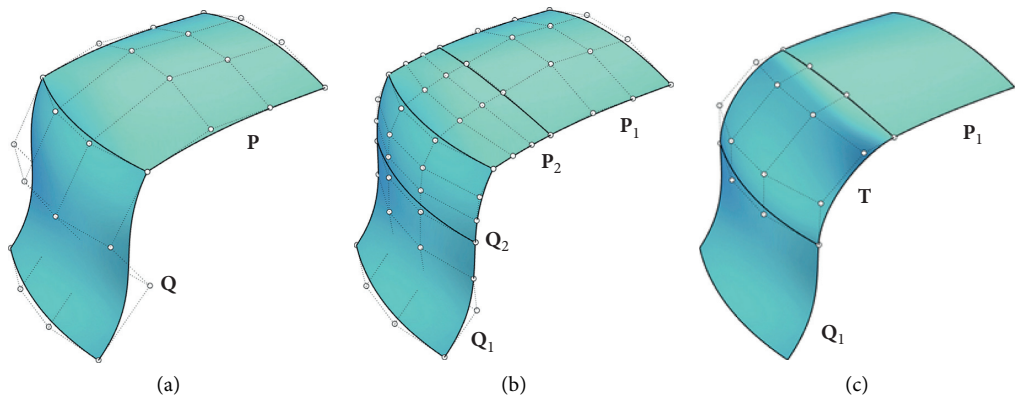


FIGURE 18: Generating a transition surface between two surfaces. (a) Surfaces **P** and **Q** with $G^0$ continuous. (b) Segmented into two surfaces $\mathbf{P}_1$, $\mathbf{P}_2$ and $\mathbf{Q}_1$, $\mathbf{Q}_2$, respectively. (c) Establishment of transition surface **T**.

*4.1. Construction of Wireframe Model Based on Feature Line.* When multi angle view is used to generate the 3D model, it is necessary to limit the drawing accuracy of each view to ensure the correctness and uniqueness of its corresponding 3D solid modeling. The sketch drawn from the designer by hand is perceptual and random, and its accuracy could not be guaranteed, especially when drawing in multiple views, which would produce errors. The length and position of the same curve in different views would be different, so the accuracy required by computer graphics could not be achieved. Therefore, it is necessary to unify the effective scope of the drawing content from multi angle view.

As shown in Figure 19(a), curves **P** and **Q** in different views are actually different angles of the same curve **S** described by the designer. However, due to the error of hand drawing, the two ends of the curves could not be aligned in different plane projections, so the actual length range of curve **S** needs to be determined first. As shown in Figure 19(b), when the two sketch 2D curves are located in *xoz* plane and *xoy* plane, respectively, the length in *x*-direction needs to be determined and unified. And the length range of the curves in *x*-direction is now set as $[x_{P1}, x_{P2}]$ and $[x_{Q1}, x_{Q2}]$, respectively; then, the length range of 3D curve **S** should be

$$[x_{S1}, x_{S2}] = [x_{P1}, x_{P2}] \cap [x_{Q1}, x_{Q2}], \tag{16}$$

which means that the *x*-direction length range of 3D curve **S** is the coincident part between the length range of 2D curves **P** and **Q** (i.e., the *x*-direction length of the cube from Figure 19(b)). By using this method, the error could be avoided to the greatest extent, and the most important part of two view 2D curve describing its shape is retained.

Then, as shown in Figure 19(c), when the effective range of two 2D sketch curves is determined, $i$ planes parallel to the *yoz* plane are generated within the range, and the *x*-coordinate set is $x_i$. These planes have $i$ intersections with curves **P** and **Q,** respectively, which are recorded as point sets $\mathbf{p}_i$ and $\mathbf{q}_i$, and their spatial coordinates are defined as $(x_i, y_p, z_p)$ and $(x_i, y_q, z_q)$. The curves **P** and **Q** could be regarded as $i-1$-degree curves interpolated at points $p_i$ and $q_i$, respectively, now. As shown in Figure 19(d), a set of point $\mathbf{r}_i$ with spatial coordinates of $(x_i, y_q, z_p)$ is generated in the space, and then the point set $\mathbf{r}_i$ is the three-dimensional point set obtained from the projection of two-dimensional point set $\mathbf{p}_i$ and $\mathbf{q}_i$ in the space actually.

Point set $\mathbf{r}_i$ is a series of interpolation points of the target curve, and the further work is to obtain its control points through its interpolation points. As shown in Figure 19(e), an $i-1$-degree curve **R** is generated by interpolation in $\mathbf{R}_i$, and then a GE-Bézier curve with $i-1$-degree whose shape parameters are valued in the middle within the range is used to simulate and merge the curve **R** to obtain its control point $\mathbf{S}_i$; finally, the curve **S** in Figure 19(f) is the final spatial 3D curve.

According to the above projection method, it is necessary to make corresponding regulations for multiview sketch. Firstly, as shown in Figure 20(a), the vehicle design scheme shall be described by drawing top view, front view, rear view, and side view. Secondly, since the 3D curve is obtained from multiview 2D curve projection, it should be ensured that any 3D structure line should be reflected in at least 2 sketches and its shape should be kept as uniform as possible. Thirdly, the structure of the whole design scheme should be designed according to the topological structure of the model CAD prototype proposed in this study, including the splicing method of each subsurface and adjacent surface. In addition, it is necessary to draw the arc curve at the hub manually and keep the bottom curve flat. Finally, the views should be arranged as shown in Figure 20(b) to ensure the correct projection relationship.

Because the car body model is a simple convex 3D structure, there is no obvious occluded curve and surface, and each modeling feature would be described by at least two views at the same time. As long as the projection relationship is determined, each 3D feature line could be generated by projection according to the method shown in Figure 19. Figure 21 describes the corresponding relationship between the curve of each view and the 3D space curve in the final model.

Finally, as shown in Figure 22, after the edge curves of each surface are established, the overall wireframe of the vehicle could be assembled. This wireframe is used as the description of the overall style of the vehicle model in the early stage of the vehicle scheme design. After that, the

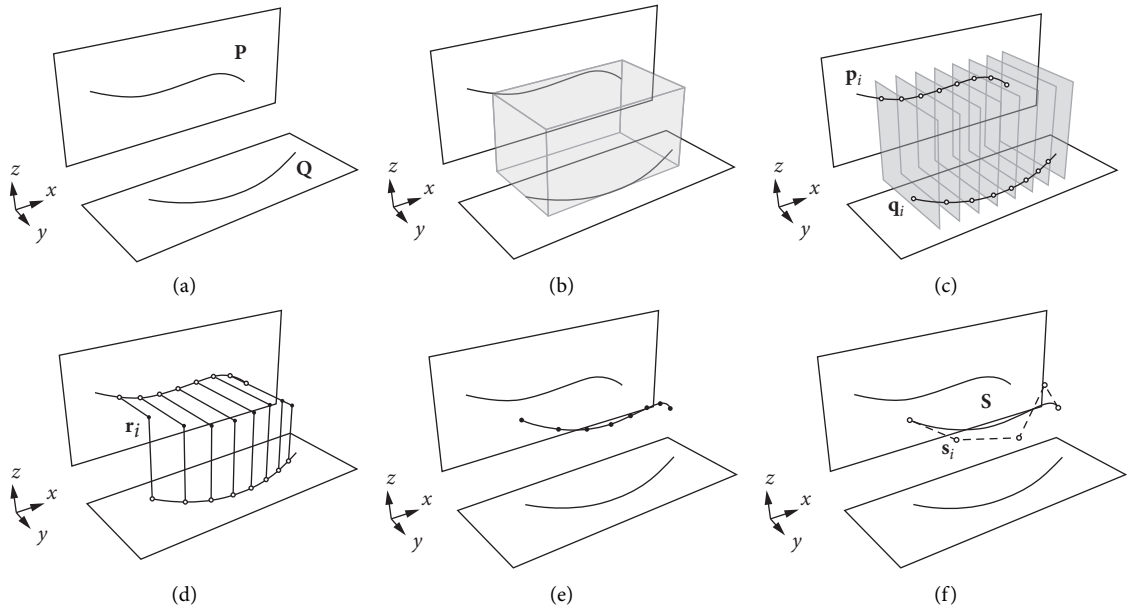


Figure 19: Determining the 3D shape of the curve by multiview plane curve. (a) Drawing two plane curves in two views. (b) Determining the size range of the 3D curve. (c) Finite planes are generated to intersect the two plane curves. (d) Generating a set of space points through two sets of intersections. (e) Generating a curve to fit the set of space points. (f) Fitting the curve with a GE-Bézier curve model.

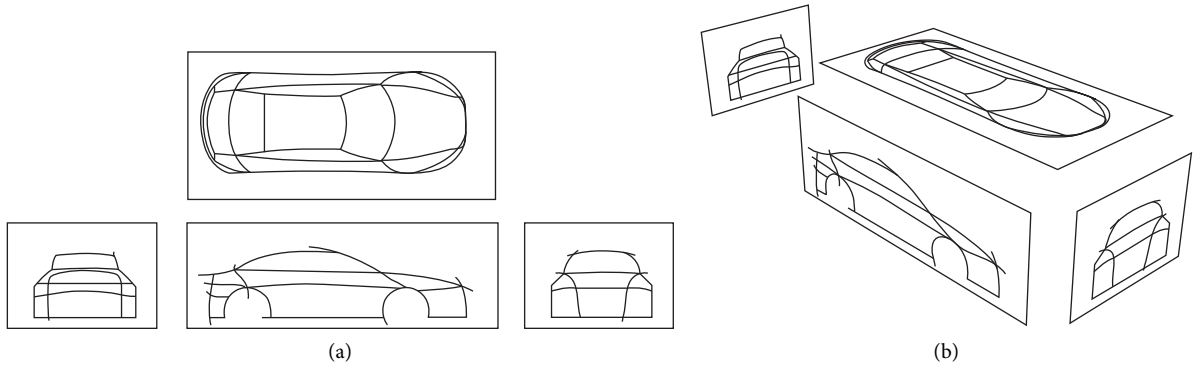


Figure 20: Multiview 2D sketch based on model template. (a) Drawing at least in four views. (b) Determining the projection relationship in 3D space.

further adjustment method could be used to further modify and adjust the vehicle appearance.

*4.2. Model Adjustment.* Because of the characteristics of extended SQ-Coons surface, as long as its shape parameters remain unchanged, its surface modeling is only controlled by the boundary curves, which has the same design concept with the car body surface modeling design method based on the characteristic curve. This also makes it an inevitable choice to modify the car body by adjusting the characteristic wireframe before transforming the 3D wireframe into specific extended SQ-Coons surface. In the adjustment process, the most basic method is that the designer directly modifies the 3D coordinates of the control points on the surface boundary curves so as to modify the overall shape of the surface. It should be noted that most of the control points in the CAD prototype template belong to the shared boundary of 2 surfaces, or the control point is the shared corner of multiple surfaces. Therefore, each adjustment of control points affects multiple surfaces.

The important significance of vehicle model adjustment is to change the dimensions and curve modeling of vehicle body in all directions. As shown in the figure, the four boundary curves of the windshield in Figure 23(a) are translated to the rear of the vehicle at the same time so as to obtain the new shape in Figure 23(b). Since the relative positions of the four boundary curves of the windshield have not changed, the shape of the windshield remains unchanged. However, because the four boundary curves are also the boundary curves of the front engine hood surface, the roof surface, and the side window surface, the movement process of the four boundary curves results in the deformation of the boundary curves of multiple surfaces (i.e., the

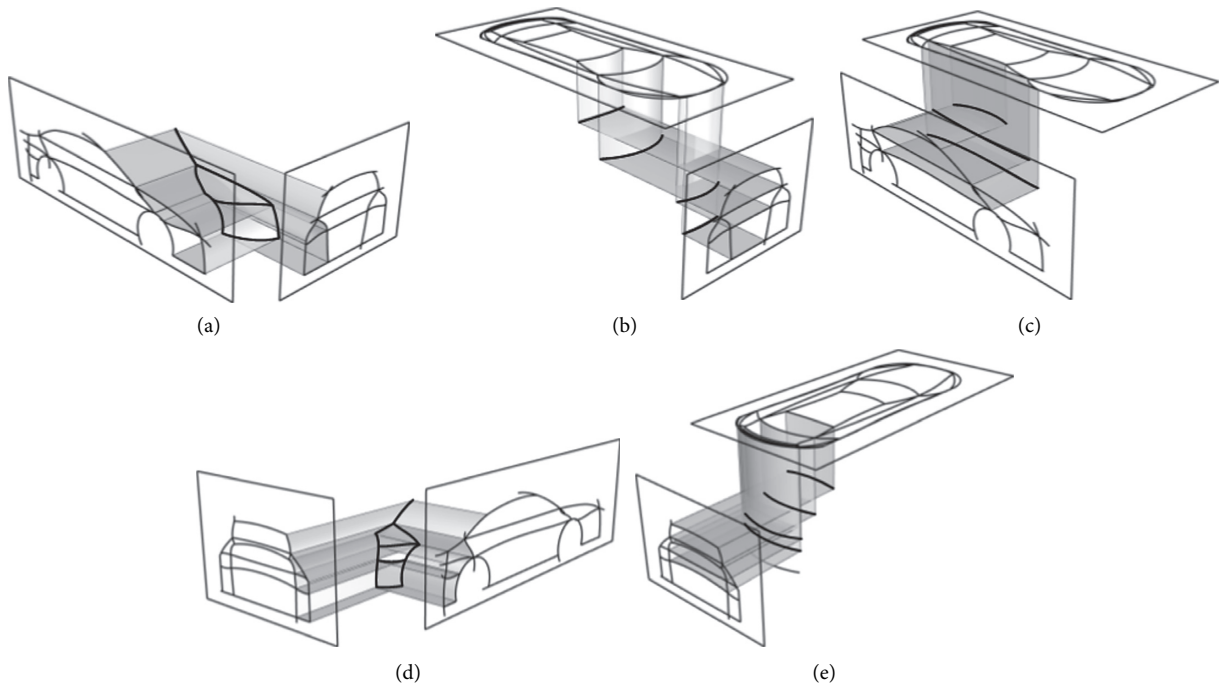


Figure 21: Relationship between each view 2D curve and the final 3D curve. (a) The front side structure line curves. (b) The structure line curves in the front of the car. (c) The structure line curves in the side of the car. (d) The rear side structure line curves. (e) The structure line curves in the rear of the car.

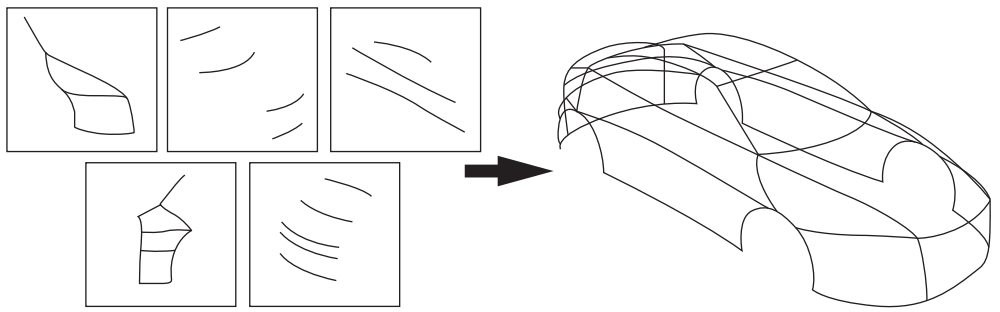

Figure 22: Establishing the whole vehicle's characteristic line with segmented 3D curves.

engine hood surface, the roof surface, and the side window surface). Since each adjustment could have similar changes involving multiple curves, this operation should be modified once the scheme is determined to avoid repeated adjustment.

As shown in Figure 24, the purpose of establishing 3D feature wireframe is to generate quadrilateral surface patches as constraints to describe and define the body surface modeling. Each closed quadrilateral curve could be used as boundary curve to generate its corresponding extended SQ-Coons surface and could be spliced according to the typical body template. After the introduction of segmentation parameters to fair the subsurfaces, the overall shape of the whole body surface would be formally constructed and established. At this time, there are still two methods to adjust the shape surface more carefully through the parameters.

*4.3. Adjustment of Transition Surface.* The significance of 3D feature line is to constrain and guide the design trend of the whole body surface. As the shared boundary curve of two surfaces, the shape of the feature line would affect the surfaces on both sides. When faired between surfaces, the shape of the transition surface could be directly adjusted by the segmentation parameters. The function of segmentation parameters is to control whether the surface transition between two surfaces is smooth or sharp without changing other design elements. In fact, the significance of the parameter value is to determine the span percentage of the target surface used to segment and generate the transition surface. The larger the span percentage is, the more surface parts are classified into the transition surface, so its visual characteristics are more smooth; on the contrary, the smaller the span percentage is, the closer it is to the undivided $G^0$ continuous state, so it is more sharp.

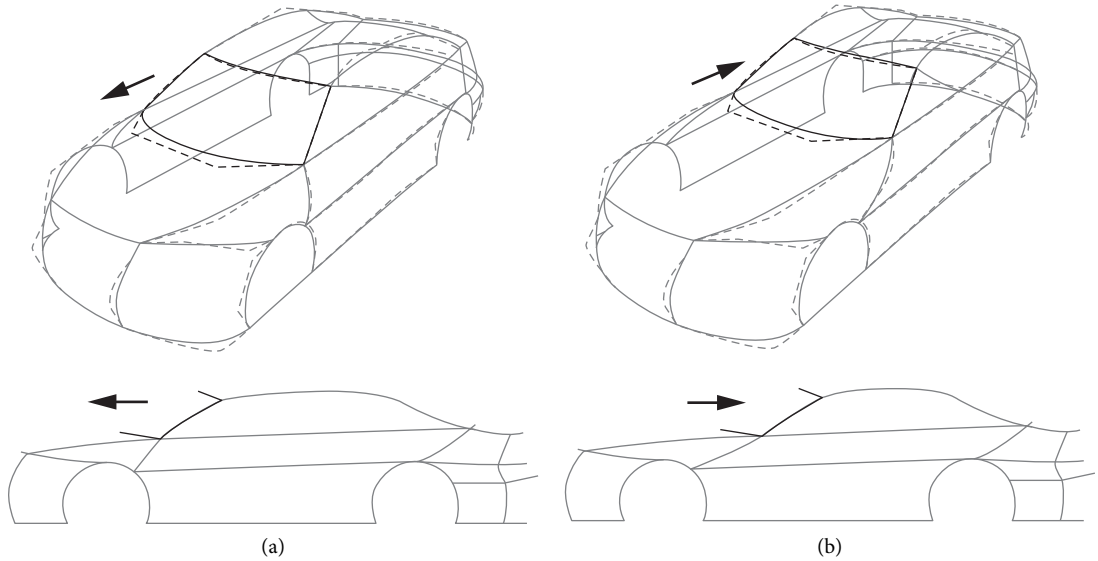


Figure 23: Position movement of the front window surface boundary. (a) Moving forward. (b) Moving backward.

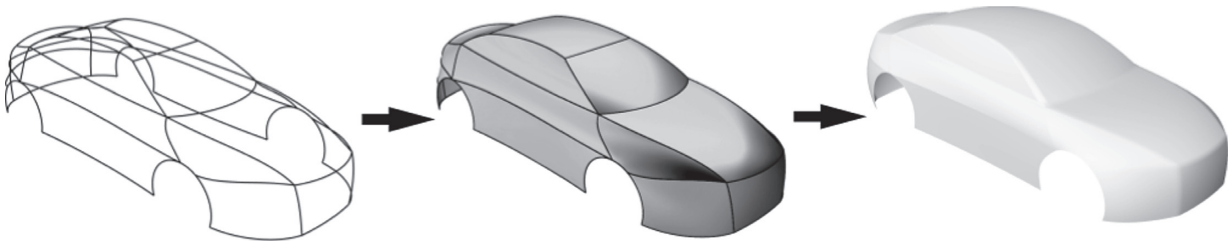

Figure 24: Generating the final body surface model from 3D feature lines.

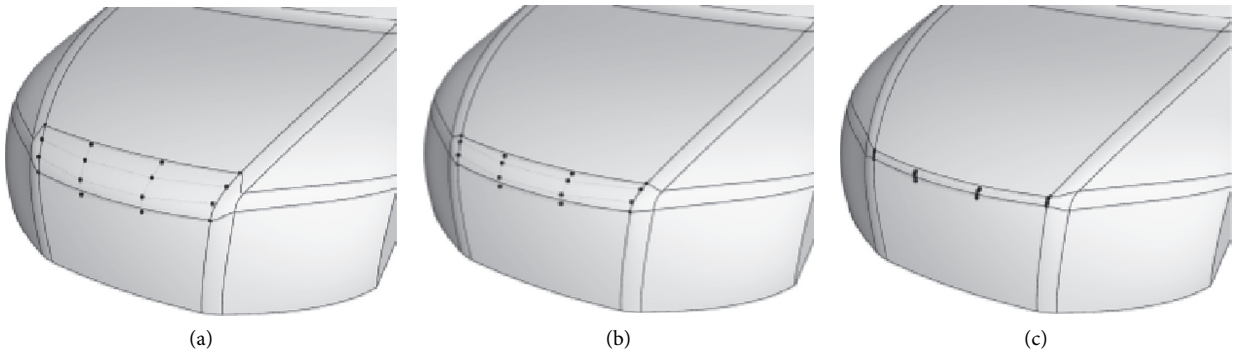


Figure 25: A transition surface and its control points with different partition parameters. (a) $u_{1\text{-}1} = 0.89$, $u_{2\text{-}0} = 0.85$. (b) $u_{1\text{-}1} = 0.94$, $u_{2\text{-}0} = 0.90$. (c) $u_{1\text{-}1} = 0.99$, $u_{2\text{-}0} = 0.95$.

Figure 25 shows that, under the premise that all other design parameters of the same vehicle model remain unchanged, only by adjusting the values of two segmentation parameters $u_{1\text{-}1}$ (the second segmentation parameter in $u$-direction of surface No. 1 in Figure 1, air intake grille surface) and $u_{2\text{-}0}$ (the first segmentation parameter in $u$-direction of surface No. 2 in Figure 1, engine hood surface), the shape of transition surface between the air intake grille subsurface and hood subsurface could be adjusted. The black dots in the figure are the control points of the transition surface. The segmentation parameters in Figure 25(a) are 0.89 and 0.85, respectively, which means that 11% and 15% of the span ratio in the intake grid subsurface and the hood subsurface on both sides of the junction curve are used for segmentation and surface fairing; as the ratio decreases in Figures 25(b) and 25(c), the segmentation ratio of the two

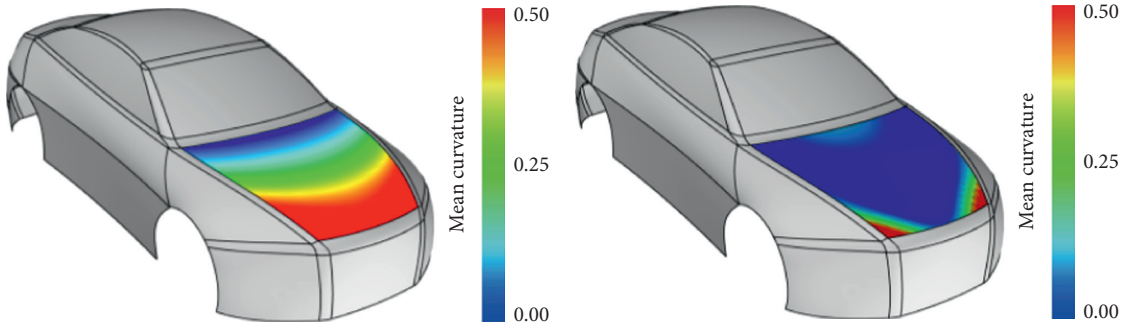


FIGURE 26: The change of the mean curvature on hood surface with different shape parameters. (a) $\alpha u, \gamma u, \alpha v, \gamma v = 1$. (b) $\alpha u, \gamma u, \alpha v, \gamma v = -3$.

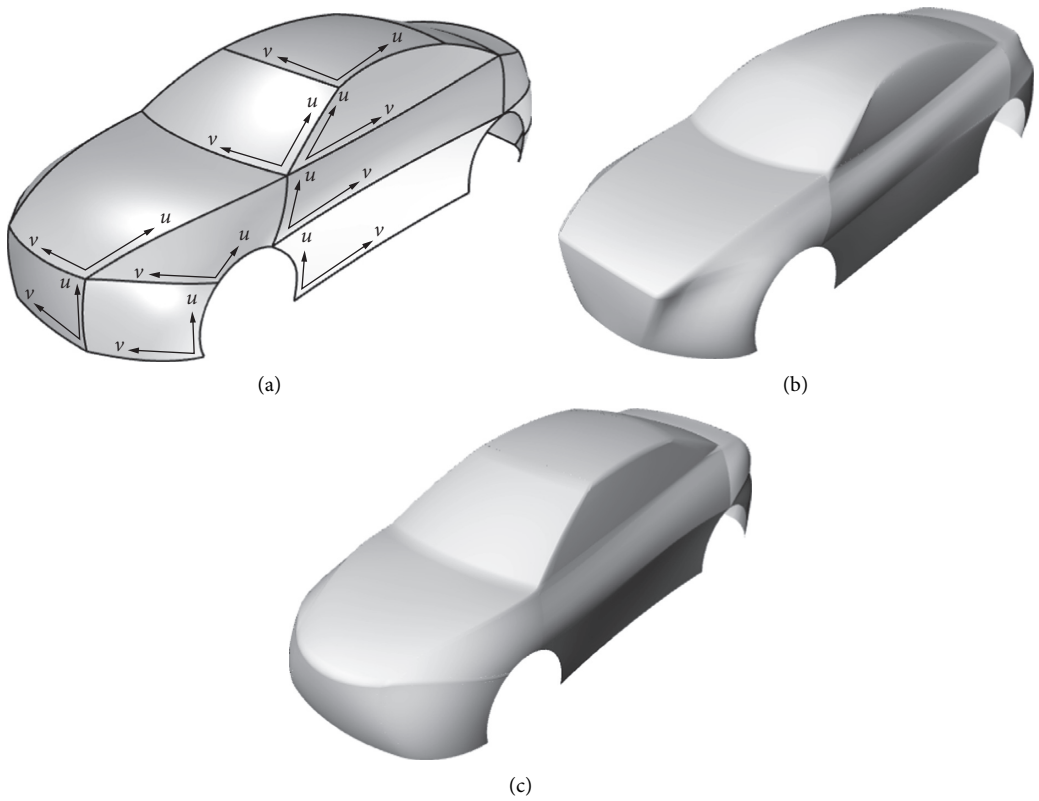


FIGURE 27: New model generation combined with the improved model template and extended SQ-Coons surfaces. (a) Template. (b) New model 1. (c) New model 2.

surfaces is smaller and more complete than the one before the parameter change. For the modeling of the transition surfaces in Figure 25, it could be seen that with the increase of the segmentation parameters, the size of the transition surface gradually reduces and the overall modeling becomes sharper. This method could be extended to the interface of any two curved surfaces in the whole body modeling template and could be controlled independently according to the position of each parameter so as to ensure that the details of this type of body meet the design requirements.

*4.4. Adjustment of Surface Details.* When the shape of the whole body and transition surfaces is determined, the details of each surface could be adjusted, and the advantages of extended SQ-Coons surface could be reflected. Because the central area of extended SQ-Coons surface could be modified by shape parameters without changing the boundary surface, the whole shape and boundary established in the previous step could not be affected in this process, and the shape of multiple surfaces could not be changed inadvertently.

Table 2: Partial surface parameter data of model template and two new models.

| Surface number | Parameter type | Model | | |
|---|---|---|---|---|
| | | Template | New model 1 | New model 2 |
| 1. Grille subsurface | Boundary curve $u0$ | (28, −388, 0) | (21, −286, 0) | (152, −566, 0) |
| | | (−9, −131, 0) | (−8, −96, 0) | (30, −201, 0) |
| | | (−9, 131, 0) | (−8, 96, 0) | (30, 201, 0) |
| | | (28, 388, 0) | (21, 286, 0) | (152, 566, 0) |
| | Boundary curve $u1$ | (67, −412, 503) | (47, −507, 529) | (160, −432, 527) |
| | | (−23, −151, 509) | (5, −172, 567) | (−28, −185, 512) |
| | | (−23, 151, 509) | (5, 172, 567) | (−28, 185, 512) |
| | | (67, 412, 503) | (47, 507, 529) | (160, 432, 527) |
| | Boundary curve $v0$ | (28, −388, 0) | (21, −286, 0) | (152, −566, 0) |
| | | (15, −388, 170) | (14, −388, 163) | (90, −499, 157) |
| | | (16, −416, 353) | (14, −452, 347) | (57, −368, 365) |
| | | (67, −412, 503) | (47, −507, 529) | (160, −432, 527) |
| | Boundary curve $v1$ | (28, 388, 0) | (21, 286, 0) | (152, 566, 0) |
| | | (15, 388, 170) | (14, 388, 163) | (90, 499, 157) |
| | | (16, 416, 353) | (14, 452, 347) | (57, 368, 365) |
| | | (67, 412, 503) | (47, 507, 529) | (160, 432, 527) |
| | Segmentation parameter | N/A | 0.00, 0.95; 0.03, 0.97 | 0.00, 0.94; 0.01, 0.99 |
| | Shape parameter | 1, 1; 1, 1 | 1, 1; 0, 0 | 0, 0; 0, 0 |
| 2. Hood subsurface | Boundary curve $u0$ | Coincident with $u1$ curve of surface 1 | | |
| | Boundary curve $u1$ | (1367, −727, 787) | (1531, −704, 808) | (1315, −725, 770) |
| | | (1173, −276, 823) | (1225, −302, 826) | (1067, −289, 856) |
| | | (1173, 276, 823) | (1225, 302, 826) | (1067, 289, 856) |
| | | (1367, 727, 787) | (1531, 704, 808) | (1315, 725, 770) |
| | Boundary curve $v0$ | (67, −412, 503) | (47, −507, 529) | (160, −432, 527) |
| | | (432, −598, 728) | (462, −711, 784) | (509, −505, 727) |
| | | (907, −696, 745) | (1026, −685, 790) | (900, −723, 757) |
| | | (1367, −727, 787) | (1531, −704, 808) | (1315, −725, 770) |
| | Boundary curve $v1$ | (1367, 727, 787) | (47, 507, 529) | (160, 432, 527) |
| | | (907, 696, 745) | (462, 711, 784) | (509, 505, 727) |
| | | (432, 598, 728) | (1026, 685, 790) | (900, 723, 757) |
| | | (67, 412, 503) | (1531, 704, 808) | (1315, 725, 770) |
| | Segmentation parameter | N/A | 0.03, 0.98; 0.02, 0.98 | 0.06, 0.94; 0.01, 0.99 |
| | Shape parameter | 1, 1; 1, 1 | 1, 1; 0, 0 | 0, 0; 0, 0 |

Table 2: Continued.

| | | | | |
|---|---|---|---|---|
| 3. Windshield subsurface | Boundary curve $u0$ | Coincident with $u1$ curve of surface 2 | | |
| | Boundary curve $u1$ | (2027, −567, 1137) | (2254, −559, 1140) | (2122, −548, 1185) |
| | | (1938, −198, 1181) | (2033, −231, 1173) | (1981, −202, 1232) |
| | | (1938, 198, 1181) | (2033, 231, 1173) | (1981, 202, 1232) |
| | | (2027, 567, 1137) | (2254, 559, 1140) | (2122, 548, 1185) |
| | Boundary curve $v0$ | (1367, −727, 787) | (1531, −704, 808) | (1315, −725, 770) |
| | | (1573, −688, 930) | (1763, −694, 946) | (1563, −663, 944) |
| | | (1793, −626, 1054) | (1998, −637, 1088) | (1836, −600, 1080) |
| | | (2027, −567, 1137) | (2254, −559, 1140) | (2122, −548, 1185) |
| | Boundary curve $v1$ | (2027, 567, 1137) | (1531, 704, 808) | (1315, 725, 770) |
| | | (1793, 626, 1054) | (1763, 694, 946) | (1563, 663, 944) |
| | | (1573, 688, 930) | (1998, 637, 1088) | (1836, 600, 1080) |
| | | (1367, 727, 787) | (2254, 559, 1140) | (2122, 548, 1185) |
| | Segmentation parameter | N/A | 0.04, 0.83; 0.04, 0.96 | 0.04, 0.93; 0.01, 0.99 |
| | Shape parameter | 1, 1; 1, 1 | 1, 1; 0, 0 | 0, 0; 0, 0 |
| 4. Roof subsurface (5 × 3-degree) | Boundary curve $u0$ | Coincident with $u1$ curve of surface 3 | | |
| | Boundary curve $u1$ | (3285, 548, 1134) | (3523, −479, 1107) | (3303, −530, 1165) |
| | | (3341, 188, 1191) | (3629, −176, 1170) | (3463, −202, 1204) |
| | | (3341, −188, 1191) | (3629, 176, 1170) | (3463, 202, 1204) |
| | | (3285, −548, 1134) | (3523, 479, 1107) | (3303, 530, 1165) |
| | Boundary curve $v0$ | (2027, −567, 1137) | (2254, −559, 1140) | (2122, −548, 1185) |
| | | (2163, −548, 1168) | (2382, −503, 1176) | (2251, −540, 1211) |
| | | (2443, −524, 1206) | (2670, −466, 1193) | (2515, −534, 1230) |
| | | (2867, −523, 1197) | (3099, −452, 1178) | (2911, −530, 1222) |
| | Boundary curve $v1$ | (3147, −538, 1158) | (3383, −466, 1138) | (3174, −530, 1192) |
| | | (3285, −548, 1134) | (3523, −479, 1107) | (3303, −530, 1165) |
| | | (2027, 567, 1137) | (2254, 559, 1140) | (2122, 548, 1185) |
| | | (2163, 548, 1168) | (2382, 503, 1176) | (2251, 540, 1211) |
| | | (2443, 524, 1206) | (2670, 466, 1193) | (2515, 534, 1230) |
| | | (2867, 523, 1197) | (3099, 452, 1178) | (2911, 530, 1222) |
| | | (3147, 538, 1158) | (3383, 466, 1138) | (3174, 530, 1192) |
| | | (3285, 548, 1134) | (3523, 479, 1107) | (3303, 530, 1165) |
| | Segmentation parameter | N/A | 0.13, 0.91; 0.02, 0.98 | 0.07, 0.93; 0.02, 0.98 |
| | Shape parameter | 1, 1, 1, 1; 1, 1 | 0, 0; 0, 0 | 0, 0; 0, 0 |

Table 2: Continued.

| | | | | |
|---|---|---|---|---|
| 10. Side window subsurface (5 × 3-degree) | Boundary curve $u0$ | (1367, −727, 787) | (1531, −704, 808) | (1315, −725, 770) |
| | | (1661, −735, 799) | (1828, −702, 782) | (1619, −724, 781) |
| | | (2248, −737, 829) | (2424, −695, 798) | (2226, −713, 820) |
| | | (3129, −699, 869) | (3315, −659, 863) | (3136, −665, 866) |
| | | (3715, −647, 879) | (3908, −614, 889) | (3743, −619, 874) |
| | | (4008, −615, 878) | (4205, −587, 890) | (4046, −594, 872) |
| | Boundary curve $u1$ | Coincident with $v0$ curve of surface 4 | | |
| | Boundary curve $v0$ | (1367, −727, 787) | (1531, −704, 808) | (1315, −725, 770) |
| | | (1573, −688, 930) | (1763, −694, 946) | (1563, −663, 944) |
| | | (1793, −626, 1054) | (1998, −637, 1088) | (1836, −600, 1080) |
| | | (2027, −567, 1137) | (2254, −559, 1140) | (2122, −548, 1185) |
| | Boundary curve $v1$ | Coincident with $v0$ curve of surface 3 | | |
| | Segmentation parameter | N/A | 0.02, 0.84; 0.01, 0.97 | 0.01, 0.89; 0.05, 0.90 |
| | Shape parameter | 1, 1; 1, 1, 1, 1 | 1, 1; 0, 0, 0, 0 | 1, 1; 1, 1, 1, 1 |
| 11. Front fender upper subsurface | Boundary curve $u0$ | (609, −916, 455) | (750, −920, 526) | (821, −887, 436) |
| | | (379, −814, 497) | (790, −875, 666) | (544, −852, 495) |
| | | (232, −596, 505) | (280, −637, 564) | (334, −643, 569) |
| | | (67, −412, 503) | (47, −507, 529) | (160, −432, 527) |
| | Boundary curve $u1$ | (1041, −916, 498) | (1155, −920, 479) | (1147, −887, 443) |
| | | (1155, −895, 610) | (1307, −919, 618) | (1191, −886, 578) |
| | | (1265, −829, 714) | (1395, −744, 700) | (1297, −792, 648) |
| | Boundary curve $v0$ | (1367, −727, 787) | (1531, −704, 808) | (1315, −725, 770) |
| | | (609, −916, 455) | (750, −920, 526) | (821, −887, 436) |
| | | (727, −916, 548) | (881, −920, 578) | (922, −887, 484) |
| | | (900, −917, 570) | (1038, −920, 560) | (1044, −887, 487) |
| | | (1041, −916, 498) | (1155, −920, 479) | (1147, −887, 443) |
| | Boundary curve $v1$ | Coincident with $v0$ curve of surface 2 | | |
| | Segmentation parameter | N/A | 0.17, 1.00; >0.00, 0.72 | 0.06, 1.00; >0.00, 0.71 |
| | Shape parameter | 1, 1; 1, 1 | 1, 1; 0, 0 | −1, −1; 1, 1 |
| 12. Front fender lower subsurface | Boundary curve $u0$ | (477, −916, 0) | (496, −920, 0) | (604, −887, 0) |
| | | (261, −809, 0) | (221, −883, 0) | (413, −870, 0) |
| | | (134, −594, 0) | (90, −540, 0) | (227, −748, 0) |
| | | (28, −388, 0) | (21, −286, 0) | (152, −566, 0) |
| | Boundary curve $u1$ | Coincident with $u0$ curve of surface 11 | | |
| | Boundary curve $v0$ | (477, −916, 5) | (496, −920, 1) | (604, −887, 0) |
| | | (416, −915, 153) | (432, −919, 207) | (568, −887, 173) |
| | | (471, −916, 352) | (547, −919, 446) | (662, −887, 360) |
| | | (609, −916, 455) | (750, −920, 526) | (821, −887, 436) |
| | Boundary curve $v1$ | Coincident with $v0$ curve of surface 1 | | |
| | Segmentation parameter | N/A | 0.00, 0.90; 0.00, 0.83 | 0.00, 0.98; 0.00, 0.93 |
| | Shape parameter | 1, 1; 1, 1 | 1, 1; 0, 0 | 0, 0; 1, |

Table 2: Continued.

| | | | | |
|---|---|---|---|---|
| 13. Side door upper subsurface ($5 \times 3$-degree) | Boundary curve $u0$ | (1041, −916, 498) | (1155, −920, 479) | (1147, −887, 443) |
| | | (1329, −899, 515) | (1452, −905, 475) | (1439, −882, 443) |
| | | (1908, −884, 539) | (2048, −874, 487) | (2023, −878, 480) |
| | | (2777, −896, 556) | (2941, −880, 529) | (2898, −880, 545) |
| | | (3356, −911, 558) | (3536, −907, 546) | (3484, −885, 520) |
| | | (3645, −916, 557) | (3834, −920, 556) | (3773, −887, 475) |
| | Boundary curve $u1$ | Coincident with $u0$ curve of surface 10 | | |
| | Boundary curve $v0$ | Coincident with $u1$curve of surface 11 | | |
| | Boundary curve $v1$ | (4008, −615, 878) | (3834, −920, 556) | (3773, −887, 475) |
| | | (3899, −755, 799) | (3967, −853, 692) | (3834, −834, 656) |
| | | (3747, −835, 697) | (4098, −755, 816) | (3957, −720, 763) |
| | | (3645, −916, 557) | (4205, −587, 890) | (4046, −594, 872) |
| | Segmentation parameter | N/A | 0.00, 0.81; 0.00, 1.00 | 0.00, 0.93; 0.00, 1.00 |
| | Shape parameter | 1, 1; 1, 1, 1, 1 | 1, 1; 1, 1, 1, 1 | 0, 0; 0, 0, 0, 0 |
| 14. Side door lower subsurface ($5 \times 3$-degree) | Boundary curve $u0$ | (1242, −916, 0) | (1321, −920, 0) | (1380, −887, 0) |
| | | (1466, −903, 0) | (1555, −919, 0) | (1602, −865, 0) |
| | | (1916, −886, 0) | (2021, −920, 0) | (2048, −843, 0) |
| | | (2590, −887, 0) | (2721, −920, 0) | (2717, −843, 0) |
| | | (3039, −904, 0) | (3188, −920, 0) | (3163, −865, 0) |
| | | (3264, −916, 0) | (3421, −920, 0) | (3385, −887, 0) |
| | Boundary curve $u1$ | Coincident with $u0$ curve of surface 13 | | |
| | Boundary curve $v0$ | (1242, −916, 5) | (1321, −920, 0) | (1380, −887, 0) |
| | | (1271, −916, 164) | (1375, −920, 174) | (1417, −887, 179) |
| | | (1319, −916, 295) | (1304, −920, 375) | (1316, −887, 372) |
| | | (1041, −916, 498) | (1155, −920, 479) | (1147, −887, 443) |
| | Boundary curve $v1$ | (3264, −916, 0) | (3421, −920, 0) | (3385, −887, 0) |
| | | (3220, −916, 203) | (3340, −920, 266) | (3336, −887, 236) |
| | | (3187, −916, 454) | (3555, −919, 557) | (3531, −887, 475) |
| | | (3645, −916, 557) | (3834, −920, 556) | (3773, −887, 475) |
| | Segmentation parameter | N/A | 0.00, 0.92; 0.00, 1.00 | 0.00, 0.95; 0.00, 1.00 |
| | Shape parameter | 1, 1; 1, 1, 1, 1 | 0, 0; 0, 0, 0, 0 | −1, −1; −1, −1, −1, −1 |

It can be seen from the properties of extended SQ-Coons surface that its adjustment degree is relatively small, and it needs to be observed from multiple angles in 3D software to perceive. Therefore, the change of mean curvature nephogram is still used to show it here. The mean curvature nephogram of the bicubic extended SQ-Coons surface of the hood from a specific vehicle model is shown in Figure 26. On the premise that the shape of the boundary curve of the surface remains unchanged, Figures 26(a) and 26(b) are different nephograms with various parameters. It can be seen that when the four parameters are all taken as 1, the curvature of the whole surface changes more smoothly and evenly; then the four shape parameters are all set to −3, and the overall curvature is more flat, but because the curvature of the front edge along the boundary curve is larger, the surface and the curve need to be interpolated, so there is a significant turning point in the front end, with a larger average curvature change rate.

*4.5. Design Example.* The above design method including multiview drawing, adjusting the 3D feature line modeling, and finally adjusting the body details through the segmentation parameters and surface shape parameters is the regular process of body modeling design through the model template and extended SQ-Coons mathematical model proposed in this paper. As shown in Figure 27, after the design method is applied to the body CAD template, the surface models of two new models are obtained through adjustment, which are named new model 1 and new model 2, respectively.

The parameters (including the prototype template, boundary curve control point coordinates, segmentation parameter values, and shape parameter values) of each subsurface in front of the body in the 3 car models are shown in Table 2. These coordinates take the center point of the lower edge of the No. 1 surface (see Figure 1) as the coordinate origin, the front to rear direction as the positive $x$-axis direction, the left to right direction of the body as the positive $y$-axis direction, and the bottom to roof direction as the positive $z$-axis direction. The boundary curve is named as boundary curve $u0$, boundary curve $u1$, boundary curve $v0$, and boundary curve $v1$ according to the $uv$ direction, and the specific $uv$ direction in each subsurface is shown in Figure 27. The coordinate unit of curve control point is mm. Most of the surfaces are bicubic surfaces, and only the surfaces of No. 4, No. 10, No. 13, and No. 14 are $5 \times 3$-degree surfaces.

It can be seen from Figure 27 and Table 2 that this design method could design and modify the automobile surface appearance parametrically. And the difference of its shape is really caused by the difference in the parameters. This also confirms the theoretical reliability of the vehicle design method proposed in this paper.

## 5. Conclusion

On the basis of the existing research, the improved car modeling template and extended SQ-Coons surface are proposed in this paper, in order to enhance their practicability in design practice. The extended SQ-Coons surface can be interpolated to boundary curve, and fine shape adjustment can be made at the same time, which provides a convenient design tool for product design based on boundary curve modeling; the improvement of the automobile form template enhances the smoothness of the surface, making it more in line with the modern aesthetic and design trends. More importantly, on the basis of all the above improvements, this paper integrates them and puts forward a set of automobile modeling design and adjustment methods. Firstly, the size and modeling features of the car are determined by hand sketching. After that, the control points of the boundary curve, segmentation parameters, and shape parameters are used in proper order to adjust the vehicle model more carefully. The final design case shows that the design method could really give full play to the advantages of extended SQ-Coons surface and use the same model template to generate vehicle appearance with completely different modeling style. This method improves the design efficiency and ensures the rationality of the design scheme.

## Data Availability

The data of surface control point coordinate and corresponding shape parameter used to support the findings of this study are included within the article.

## Conflicts of Interest

The authors declare that there are no conflicts of interest regarding the publication of this paper.

## Acknowledgments

This study was supported by the General Special Scientific Research Plan of Shaanxi Provincial Education Department in China (no. 20JK0070), National Natural Science Foundation of China (no. 51875454), and Postgraduate Training Project from Xi'an University of Technology (no. 252051626).

## References

[1] Y. Bodein, B. Rose, and E. Caillaud, "A roadmap for parametric CAD efficiency in the automotive industry," *Computer-Aided Design*, vol. 45, no. 10, pp. 1198–1214, 2013.

[2] H. Prautzsch, W. Boehm, and M. Paluszny, *Bézier and B-Spline Techniques*, Springer Science & Business Media, New York, NY, USA, 2002.

[3] Q. W. Guo, J. Xiong, and G. Q. Zhu, "Extensions of C-Bézier curves and surfaces," *Computer Engineering and Applications*, vol. 45, no. 12, pp. 170–173, 2009.

[4] X.-A. Han, X. Huang, and Y. Ma, "Shape analysis of cubic trigonometric Bézier curves with a shape parameter," *Applied Mathematics and Computation*, vol. 217, no. 6, pp. 2527–2533, 2010.

[5] X. Qin, G. Hu, Y. Yang, and G. Wei, "Construction of PH splines based on H-Bézier curves," *Applied Mathematics and Computation*, vol. 238, no. 1, pp. 460–467, 2014.

[6] Z. Liu, X. Chen, and P. Jiang, "A class of generalized bézier curves and surfaces with multiple shape parameters," *Journal of Computer-Aided Design & Computer Graphics*, vol. 22, no. 5, pp. 838–844, 2010.

[7] L. Yang and X.-M. Zeng, "Bézier curves and surfaces with shape parameters," *International Journal of Computer Mathematics*, vol. 86, no. 7, pp. 1253–1263, 2009.

[8] K. Ri, "Bézier curves with multi-shape-parameters," *Journal of Zhejiang University (Science Edition)*, vol. 37, no. 4, pp. 401–405, 2010, in Chinese.

[9] X. Q. Qin, G. Hu, and S. X. Zhang, "New extension of cubic Bézier curve and its applications," *Computer Engineering and Applications*, vol. 44, no. 2, pp. 112–115, 2008, in Chinese.

[10] X. Qin, G. Hu, N. Zhang, X. Shen, and Y. Yang, "A novel extension to the polynomial basis functions describing Bezier curves and surfaces of degree n with multiple shape parameters," *Applied Mathematics and Computation*, vol. 223, pp. 1–16, 2013.

[11] G. Hu, J. Wu, and X. Qin, "A novel extension of the Bézier model and its applications to surface modeling," *Advances in Engineering Software*, vol. 125, pp. 27–54, 2018.

[12] W. Shen and G. Wang, "Geometric shapes of C-Bézier curves," *Computer-Aided Design*, vol. 58, pp. 242–247, 2015.
[13] G. Hu, C. C. Bo, J. L. Wu, G. Wei, and F. Hou, "Modeling of free-form complex curves using SG-Bézier curves with constraints of geometric continuities," *Symmetry*, vol. 10, no. 11, p. 545, 2018.
[14] G. Hu, H. X. Cao, and S. X. Zhang, "Approximate multidegree reduction of $\lambda$-Bézier curves," *Mathematical Problems in Engineering*, vol. 2016, Article ID 061102, 12 pages, 2016.
[15] G. Hu, X. M. Ji, X. Q. Qin, and S. X. Zhang, "Shape modification for $\lambda$-Bézier curves based on constrained optimization of position and tangent vector," *Mathematical Problems in Engineering*, vol. 2015, Article ID 735629, 12 pages, 2015.
[16] G. Hu, J. Wu, and X. Qin, "A new approach in designing of local controlled developable H-Bézier surfaces," *Advances in Engineering Software*, vol. 121, pp. 26–38, 2018.
[17] H. Li, X. Qin, D. Zhao, J. Chen, and P. Wang, "An improved empirical mode decomposition method based on the cubic trigonometric B-spline interpolation algorithm," *Applied Mathematics and Computation*, vol. 332, pp. 406–419, 2018.
[18] T. Nazir, M. Abbas, A. I. M. Ismail, A. A. Majid, and A. Rashid, "The numerical solution of advection–diffusion problems using new cubic trigonometric B-splines approach," *Applied Mathematical Modelling*, vol. 40, no. 7-8, pp. 4586–4611, 2016.
[19] Y. Zhu and X. Han, "A class of $\alpha\beta\gamma$-Bernstein-Bézier basis functions over triangular domain," *Applied Mathematics and Computation*, vol. 220, pp. 446–454, 2013.
[20] G. Hu, H. Cao, S. Zhang, and G. Wei, "Developable Bézier-like surfaces with multiple shape parameters and its continuity conditions," *Applied Mathematical Modelling*, vol. 45, pp. 728–747, 2017.
[21] U. Bashir, M. Abbas, and J. M. Ali, "The G2 and C2 rational quadratic trigonometric Bézier curve with two shape parameters with applications," *Applied Mathematics and Computation*, vol. 219, no. 20, pp. 10183–10197, 2013.
[22] G. Xu and G.-Z. Wang, "AHT bézier curves and NUAHT B-spline curves," *Journal of Computer Science and Technology*, vol. 22, no. 4, pp. 597–607, 2007.
[23] C. Xie, J. C. Li, Y. E. Zhong, L. Yang, and C. Y. Liu, "Trigonometric coons patch with shape parameters," *Advanced Materials Research*, vol. 482–484, pp. 595–598, 2012.
[24] J. X. Wang, Y. Dong, and J. Ni, "Biquadrate trigonometric polynomial Coons patch with adjustable parameters," *Journal of Dalian Jiaotong University*, vol. 34, no. 1, pp. 110–112, 2013, in Chinese.
[25] Q. Pei, L. Li, and Y. Li, "Modal parameter identification of civil engineering structures under seismic excitations," *Advanced Materials Research*, vol. 859, no. 10, pp. 163–166, 2013, in Chinese.
[26] Q. Zou, "Coons surfaces based on rational blending function with shape parameters and its properties," *Journal of Huaibei Normal University (Natural Science Edition)*, vol. 34, no. 2, pp. 6–9, 2013, in Chinese.
[27] L. Piegl and W. Tiller, *The NURBS Book*, Springer-Verlag, New York, NY, USA, 2nd edition, 1997.
[28] Y.-J. Liu, K. Tang, W.-Y. Gong, and T.-R. Wu, "Industrial design using interpolatory discrete developable surfaces," *Computer-Aided Design*, vol. 43, no. 9, pp. 1089–1098, 2011.
[29] S.-W. Hsiao and H.-C. Tsai, "Applying a hybrid approach based on fuzzy neural network and genetic algorithm to product form design," *International Journal of Industrial Ergonomics*, vol. 35, no. 5, pp. 411–428, 2005.
[30] R. Vignesh, R. Suganthan, and K. Prakasan, "Development of CAD models from sketches: a case study for automotive applications," *Proceedings of the Institution of Mechanical Engineers, Part D: Journal of Automobile Engineering*, vol. 221, no. 1, pp. 41–47, 2007.
[31] E. Gunpinar and S. Gunpinar, "A shape sampling technique via particle tracing for CAD models," *Graphical Models*, vol. 96, pp. 11–29, 2018.
[32] V. Cheutet, C. E. Catalano, J. P. Pernot et al., "3D sketching for aesthetic design using fully free-form deformation features," *Computers and Graphics*, vol. 29, no. 6, pp. 916–930, 2005.
[33] J. Guo, F. Ding, X. Jia, and D.-M. Yan, "Automatic and high-quality surface mesh generation for CAD models," *Computer-Aided Design*, vol. 109, pp. 49–59, 2019.
[34] J.-B. Bluntzer, E. Ostrosi, and J.-C. Sagot, "Car styling: a CAD approach to identify, extract and interpret characteristic lines," *Procedia CIRP*, vol. 21, pp. 258–263, 2014.
[35] E. Ostrosi, J.-B. Bluntzer, Z. Zhang, and J. Stjepandić, "Car style-holon recognition in computer-aided design," *Journal of Computational Design and Engineering*, vol. 6, no. 4, pp. 719–738, 2019.
[36] Y. Xiong, Y. Li, P. Y. Pan, and Y. Chen, "A regression-based Kansei engineering system based on form feature lines for product form design," *Advances in Mechanical Engineering*, vol. 8, no. 7, pp. 1–12, 2016.
[37] B. Kumar and P. Sarkar, "Prediction of future car forms based on historical trends," *Perspectives in Science*, vol. 8, pp. 764–766, 2016.
[38] F. Cluzel, B. Yannou, and M. Dihlmann, "Using evolutionary design to interactively sketch car silhouettes and stimulate designer's creativity," *Engineering Applications of Artificial Intelligence*, vol. 25, no. 7, pp. 1413–1424, 2012.
[39] K. H. Hyun, J.-H. Lee, M. Kim, and S. Cho, "Style synthesis and analysis of car designs for style quantification based on product appearance similarities," *Advanced Engineering Informatics*, vol. 29, no. 3, pp. 483–494, 2015.